The Journal of Immunology

This information is current as of December 12, 2016.

Airway Epithelial KIF3A Regulates Th2 Responses to Aeroallergens

Premkumar Vummidi Giridhar, Sheila M. Bell, Anusha Sridharan, Priya Rajavelu, Joseph A. Kitzmiller, Cheng-Lun Na, Matthew Kofron, Eric B. Brandt, Mark Ericksen, Anjaparavanda P. Naren, Changsuk Moon, Gurjit K. Khurana Hershey and Jeffrey A. Whitsett

J Immunol 2016; 197:4228-4239; Prepublished online 28 October 2016;
doi: 10.4049/jimmunol.1600926
http://www.jimmunol.org/content/197/11/4228

Supplementary Material **http://www.jimmunol.org/content/suppl/2016/10/27/jimmunol.1600926.DCSupplemental.html**

References This article **cites 69 articles**, 22 of which you can access for free at:
http://www.jimmunol.org/content/197/11/4228.full#ref-list-1

Subscriptions Information about subscribing to *The Journal of Immunology* is online at:
http://jimmunol.org/subscriptions

Permissions Submit copyright permission requests at:
http://www.aai.org/ji/copyright.html

Email Alerts Receive free email-alerts when new articles cite this article. Sign up at:
http://jimmunol.org/cgi/alerts/etoc

The Journal of Immunology is published twice each month by
The American Association of Immunologists, Inc.,
9650 Rockville Pike, Bethesda, MD 20814-3994.
Copyright © 2016 by The American Association of Immunologists, Inc. All rights reserved.
Print ISSN: 0022-1767 Online ISSN: 1550-6606.

Downloaded from http://www.jimmunol.org/ at Liverpool University Library on December 12, 2016

Airway Epithelial KIF3A Regulates Th2 Responses to Aeroallergens

Premkumar Vummidi Giridhar,* Sheila M. Bell,* Anusha Sridharan,* Priya Rajavelu,* Joseph A. Kitzmiller,* Cheng-Lun Na,* Matthew Kofron,† Eric B. Brandt,‡ Mark Ericksen,‡ Anjaparavanda P. Naren,§ Changsuk Moon,§ Gurjit K. Khurana Hershey,‡ and Jeffrey A. Whitsett*

***KIF3A*, the gene encoding kinesin family member 3A, is a susceptibility gene locus associated with asthma; however, mechanisms by which KIF3A might influence the pathogenesis of the disorder are unknown. In this study, we deleted the mouse *Kif3a* gene in airway epithelial cells. Both homozygous and heterozygous *Kif3a* gene–deleted mice were highly susceptible to aeroallergens from *Aspergillus fumigatus* and the house dust mite, resulting in an asthma-like pathology characterized by increased goblet cell metaplasia, airway hyperresponsiveness, and Th2-mediated inflammation. Deletion of the *Kif3a* gene increased the severity of pulmonary eosinophilic inflammation and expression of cytokines (*Il-4*, *Il-13*, and *Il-17a*) and chemokine (*Ccl11*) RNAs following pulmonary exposure to *Aspergillus* extract. Inhibition of *Kif3a* disrupted the structure of motile cilia and impaired mucociliary clearance, barrier function, and epithelial repair, demonstrating additional mechanisms by which deficiency of KIF3A in respiratory epithelial cells contributes to pulmonary pathology. Airway epithelial KIF3A suppresses Th2 pulmonary inflammation and airway hyperresponsiveness following aeroallergen exposure, implicating epithelial microtubular functions in the pathogenesis of Th2-mediated lung pathology. *The Journal of Immunology*, 2016, 197: 4228–4239.**

Asthma is an increasingly common, complex pulmonary disorder causing reversible airflow obstruction, mucus hyperproduction, and inflammation. Both environmental and genetic factors are associated with risk of asthma. Although allergic asthma is often associated with atopy and Th2 immune activation, expression of IL-13, IL-4, and IL-5, and eosinophilic pulmonary inflammation (1), there is substantial heterogeneity in asthma phenotypes among patient populations. For example, Th1 activation is associated with obesity and asthma (2). Th2-related asthma patients can be further subdivided on the basis of increased Th2 cytokine and periostin expression, neutrophilic inflammation, and responses to inhaled steroids, indicating that the heterogeneity of asthma phenotypes is highly relevant to therapeutic responses (3–5). Environmental exposures to pollutants, respiratory viruses, allergens, and bacterial and fungal products are known to play important roles in the pathogenesis of asthma (for review, see Edwards et al. and Parnia et al. [6, 7]). Likewise, a number of genetic factors influence susceptibility and severity of asthma. Extensive genome-wide analyses from diverse populations identified numerous haplotypes and chromosomal loci associated with asthma and atopy, with both allergic rhinitis and eczema being closely associated with increased risk of childhood asthma. Genome-wide association studies identified increased susceptibility to asthma associated with variations in genes controlling inflammation, including genes regulating Th2 lymphocyte recruitment and activation (e.g., *IL-33*, *ST2*, *TSLP*, *ORMDL3*, *GSDML*, *ADAM33*, *SPINK5*) that were associated with asthma susceptibility (8, 9). Polymorphisms in FCεRI-β, a high-affinity receptor for IgE on mast cells, was linked to childhood asthma and allergic dermatitis (10).

The human *KIF3A* gene locus has been repeatedly implicated in susceptibility to asthma and eczema (11–16). KIF3A, a member of the kinesin-2 family, is a component of a trimeric motor complex regulating microtubular function and transport and is required for formation and function of both motile cilia and nonmotile primary and sensory cilia (17, 18). KIF3A plays pleiotropic roles in the regulation of microtubular transport, influencing intracellular protein trafficking, as well as ciliary transport and function (17–19). Genomic deletion of *Kif3a* in the mouse is embryonically lethal (20–22). In the lung, motile cilia occur as clusters on apical surfaces of ciliated cells that coordinate mucociliary clearance in the airways. Whereas primary cilia are singular, nonmotor organelles present on many cell types, including pulmonary cells, that are known to mediate signal transduction through diverse signaling pathways, including Shh, Wnt, Pdgf, and others, influencing morphogenesis, homeostasis, and repair of many organs (23–26). In various experimental models, roles for KIF3A in the regulation of cell proliferation, apoptosis, differentiation, intracellular transport, cytoskeletal dynamics, and planar polarity have been demonstrated (27–31).

*Division of Neonatology, Perinatal and Pulmonary Biology, Perinatal Institute, Cincinnati Children's Hospital Medical Center, Cincinnati, OH 45229; †Division of Developmental Biology, Perinatal Institute, Cincinnati Children's Hospital Medical Center, Cincinnati, OH 45229; ‡Division of Asthma Research, Perinatal Institute, Cincinnati Children's Hospital Medical Center, Cincinnati, OH 45229; and §Division of Pulmonary Medicine, Perinatal Institute, Cincinnati Children's Hospital Medical Center, Cincinnati, OH 45229

ORCIDs: 0000-0001-9029-7407 (P.V.G.); 0000-0003-2771-8306 (C.-L.N.); 0000-0003-0617-4100 (E.B.B.); 0000-0003-2834-051X (A.P.N.); 0000-0001-6663-977X (G.K.K.H.).

Received for publication May 31, 2016. Accepted for publication October 3, 2016.

This work was supported by National Institutes of Health Grants R01 HL095580, R01 HL110964 (both to J.A.W.), and 2U19AI070235-11 (to G.K.K.H.).

Address correspondence and reprint requests to Dr. Jeffrey A. Whitsett, Division of Pulmonary Biology, MLC7029, Cincinnati Children's Hospital Medical Center, 3333 Burnet Avenue, Cincinnati, OH 45229-3039. E-mail address: jeff.whitsett@cchmc.org

The online version of this article contains supplemental material.

Abbreviations used in this article: ACTA2, α_2–smooth muscle actin; ac-TUBA4A, acetylated α-tubulin; AHR, airway hyperresponsiveness; BALF, bronchoalveolar lavage fluid; E, embryonic day; EpCAM, epithelial cell adhesion molecule; HDM, house dust mite; IFT88, intraflagellar transporter protein 88; i.t., intratracheal(ly); qRT-PCR, quantitative RT-PCR; shRNA, short hairpin RNA.

Copyright © 2016 by The American Association of Immunologists, Inc. 0022-1767/16/$30.00

Downloaded from http://www.jimmunol.org/ at Liverpool University Library on December 12, 2016

Although *KIF3A* gene polymorphisms have been correlated with asthma, allergic rhinitis, and eczema, cellular mechanisms underlying this association are unknown. In the present study, we selectively deleted the mouse *Kif3a* gene in airway epithelial cells. Loss of *Kif3a* enhanced pulmonary inflammation, airway hyperresponsiveness (AHR), and Th2-mediated inflammation following aeroallergen challenge with *Aspergillus fumigatus* and house dust mite (HDM) extracts. KIF3A was required for mucociliary clearance, epithelial cell migration, and repair, providing plausible mechanisms by which KIF3A influences susceptibility to asthma.

Materials and Methods

Mice

Animal protocols were approved by the Institutional Animal Care and Use Committee in accordance with National Institutes of Health guidelines. $Kif3a^{fl/fl}$ mice, generated by Marszalek et al. (21) and Lin et al. (20), and intraflagellar transporter protein 88 $(Ift88)^{fl/fl}$ mice generated by Haycraft et al. (32) were provided by S.A. Brugmann (Department of Plastic Surgery, Cincinnati Children's Hospital Medical Center). *Scgb1a1-Cre* mice were provided by Dr. S. Shapiro (33). $Gt(ROSA)26Sor^{tm4(ACTB-tdTomato,-EGFP)Luo}$/J and $Shh^{tm1(EGFP/Cre)Cjt}$/J (34) mice were purchased from The Jackson Laboratory.

Naphthalene injury

Mice were administered naphthalene (30 mg/ml in corn oil; Sigma-Aldrich, St. Louis, MO) via a single i.p. injection to deliver a dose of 275 μg/g body weight. Control animals were injected with corn oil. Animals were sacrificed at 2, 7, and 10 d after administration.

Aspergillus *and HDM extract sensitization*

Anesthetized 6- to 8-wk-old mice were administered a dose of 10 μg of *A. fumigatus* or HDM extract (25 μg) (Greer Laboratories, Lenoir, NC) diluted in 50 μl of saline by intratracheal (i.t.) instillation three times weekly for 3 wk. Control animals were dosed with saline. Mice were sacrificed 48 h following the last exposure.

AHR/flexiVent

Airway responsiveness of anesthetized mice was assessed with a flexiVent apparatus (Scireq, Montreal, QC, Canada) using an invasive method. Mice were anesthetized and the tracheas cannulated with an 18-gauge blunt needle. Mice were ventilated at 150 breaths/min, 3 cm of water positive end-expiratory pressure. Two total lung capacity perturbations were performed for airway recruitment before baseline measurement and subsequent methacholine challenges were performed. Acetyl-β-methacholine chloride (Sigma-Aldrich) was administered for 10 s (60 breaths/min, 500-μl tidal volume) in increasing concentrations (12.5, 25, and 50 mg/ml) via nebulization via the tracheotomy. Dynamic resistance (R) was determined by fitting the data to a single compartment model of airway mechanics where $P_{tr} = RV + EV + P_O$ (P_{tr}, tracheal pressure; V, volume; and P_O, constant). The average of the three highest R values with a coefficient of ≥0.9 was used to plot the dose-response curves.

Bronchoalveolar lavage fluid

Bronchoalveolar lavage fluid (BALF) was collected from the right lobes by lavage (three times with 0.7 ml of normal saline). BALF was centrifuged and cell pellets were resuspended in HBSS, and total cell numbers were counted using a hemocytometer. Cytospins were prepared and stained with a Diff-Quik staining kit (Polysciences, Warrington, PA) to determine differential cell counts.

Histology and immunohistochemistry

Mouse lungs were inflation fixed in 4% paraformaldehyde in PBS overnight. Fixed tissue was processed according to standard protocols for paraffin embedding and used for chemical or immunohistochemical staining. Depending on the primary Ab, some sections were subjected to Ag retrieval using citrate buffer (pH 6) or 10 mM Tris-EDTA buffer (pH 9) with heating. For in vitro studies, cells grown on ibiTreat chambered coverslips (ibidi) were fixed with 4% paraformaldehyde/PBS for 15 min and permeabilized with 0.2% Triton X-100 in PBS for 7 min at room temperature. Primary Abs were applied overnight at 4˚C. Primary Abs used were acetylated α-tubulin (T7451, 1:3000; Sigma-Aldrich), ARL13B (17711-1-AP, 1:200; Proteintech), E-cadherin (3195, 1:100; Cell Signaling Technology), FOXJ1 (1409965-82, 1:200; eBioscience), FOXA3 (sc-5361, 1:50; Santa Cruz Biotechnology), MUC5AC (Ab3649, 1:100; Abcam), SCGB1A1 (1:800; CCHMC), α_2–smooth muscle actin (ACTA2; A5228, 1:2000; Sigma-Aldrich), TUBB4A (MU178-UC, 1:200; Biogenex), α-tubulin (T6199, 1:200; Sigma-Aldrich), and phospho–histone H3 (sc-8656-R, 1:100; Santa Cruz Biotechnology). FOXJ1 and FOXA3 were detected with species-specific biotinylated secondary Abs and then visualized with a streptavidin-conjugated fluorophore. For all other Abs, fluorophore-conjugated secondary Abs were used, including Alexa Fluor 488, Alexa Fluor 555, Alexa Fluor 568, Alexa Fluor 594, and Alexa Fluor 647 (Jackson ImmunoResearch Laboratories and Life Technologies). For fluorescence stains, sections were stained with DAPI and mounted with ProLong Gold anti-fade reagent (Life Technologies). Bright-field images were obtained using a Zeiss Axio Imager A2 microscope equipped with AxioVision software. Confocal immunofluorescence images were obtained using a Nikon A1Rsi inverted laser confocal microscope, and wide-field images were obtained using a Nikon Ti-E inverted microscope equipped with an Andor Zyla 4.2 sCMOS camera. Images were analyzed using NIS-Elements (Nikon) or Imaris (Bitplane) software.

Scanning electron microscopy

Three mouse lungs from each genotype were inflation fixed with ice-cold 2% paraformaldehyde, 2% glutaraldehyde in 0.1 M sodium cacodylate buffer (pH 7.3) for 30 min, followed by postfixation with fresh fixative at 4˚C overnight. Fixed mouse lungs were sliced into 1- to 2-mm slabs, incubated with 1% osmium and 1.5% potassium ferrocyanide in 0.1 M sodium cacodylate buffer (pH 7.3) for 2 h, dehydrated in a graded series of alcohol, washed with hexamethyldisilazane, and air dried in a chemical fume hood for up to 2 d. Mouse lung tissue slabs were mounted on specimen stubs and coated with palladium/gold film using a Denton Vacuum Desk IV sputter coater. Scanning electron micrographs of murine airways were acquired using a Hitachi field emission scanning electron microscope SU8010 at 5 kV.

Mouse trachea and airway sample preparation and video microscopy for ciliary beat and mucociliary clearance

Three mice of each genotype (control, heterozygote, or homozygote) from the $Kif3a^{Shh}$ or $Kif3a^{Scg}$ lines were analyzed. Tracheas and lungs from the $Kif3a^{Scg\Delta/\Delta}$ mice were prepared as described (35). Tracheas from $Kif3a^{Shh\Delta/\Delta}$ mice and controls were removed, washed, and prepared according to Francis and Lo (36). For clearance assays, samples were placed on a glass dish in medium containing 0.20-μm Fluoresbrite microspheres (Polysciences). Ciliary dynamics were captured with a ×40 objective using differential interference contrast on a Nikon Ti-E inverted microscope equipped with a Andor Zyla 4.2 sCMOS camera or with the ×60 objective using differential interference contrast on an Olympus 1X51 inverted microscope equipped with a Hamamatsu EM-CCD digital camera. Images up to 500 frames/s were recorded. To quantitate ciliary beat frequency and cilia-generated flow, at least two videos were collected from each tracheal sample (n = 3 per genotype). Using ImageJ software (National Institutes of Health), a line was marked perpendicular to the cilia captured in each video and a kymograph was created. The number of pixels between each wave peak was measured (one pixel = one video frame) from which the number of beats per minute (i.e., Hertz) was calculated. To measure cilia-generated flow, MTrackJ ImageJ software was used to manually track fluorescence beads across the surface of the tracheal epithelia.

RNA isolation and analysis

Total RNA was isolated from snap-frozen left lung lobes using a tissue homogenizer (OMNI-TH; Omni International, Kennesaw, GA) by pulsing the probe for ~20 s in 1 ml of TRIzol reagent (Life Technologies) and extracting the RNA using Direct-zol RNA MiniPrep R2072 (Zymo Research, Irvine, CA). RNA was isolated from purified epithelial cells and cells in culture using a Qiagen RNeasy micro kit (Qiagen, Valencia, CA, catalog no. 74004). RNA cleanup and on-column DNase digestion (Qiagen RNeasy micro kit) was performed on samples before being reverse transcribed either with a first-strand SuperScript synthesis kit (Invitrogen) or iScript cDNA synthesis kit (Bio-Rad). Quantitative real-time PCR analysis was performed on cDNA samples using TaqMan probes (Applied Biosystems) (Table I) and *EUK 18S rRNA* (4352930), *FoxJ1* (Mm00807215_m1), *Arl13b* (Mm01349328_m1), *Kif3a* (Mm01288585_m1), *KIF3A* (Hs00199901_m1), and *CDH1* (Hs01023894_m1) on an ABI 2720 thermal cycler (Applied Biosystems).

Lung cell isolation and epithelial cell adhesion molecule sorting

Lung tissues were enzymatically digested at 37˚C for 1 h using Dispase (Discovery Labware; Corning, Bedford, MA). After 1 h, DNaseI was added prior to passing the solution through a 19-gauge needle to remove tissue

Downloaded from http://www.jimmunol.org/ at Liverpool University Library on December 12, 2016

aggregates. Cells were resuspended in MACS buffer and cell counts determined. For every 1×10^7 cells of lung suspension, 10 μl of epithelial cell adhesion molecule (EpCAM)–biotin Ab (CD326 EpCAM-biotin, 130-101-859, MACS; Miltenyi Biotec) was added. Cells were incubated with primary Ab for 15 min at 4°C, washed and resuspended in MACS buffer, and incubated with the secondary Ab (streptavidin-conjugated microbeads 130-048-102) for selection of epithelial cells. $EpCAM^+$ cells were collected by magnetic separation using an autoMACS (Miltenyi Biotec).

In vitro assays

HBEC3 cells (a kind gift of Dr. J.D. Minna, University of Texas Southwestern Medical Center) and BEAS-2B (American Type Culture Collection) cells were grown to confluence on 12-well tissue culture plates (TPP Techno Plastic Products plasticware). At 48 h after plating, the cells were infected with lentiviral constructs expressing short hairpin RNA (shRNA) against *KIF3A* or scramble controls (multiplicity of infection of 2) in the presence of Polybrene (2 μg/ml; Sigma-Aldrich) to determine cell migration and motility. The cells were stained at 72 h after transduction with di-8-ANEPPS (Biotium) diluted 1:500 in culture media. A scratch was made in each well of the plate using a p200 pipette tip. The cells were washed with 1× PBS and fed with culture media containing di-8-ANEPPS. For rescue experiments, HBEC3 transduced with lentiviral cells or scramble control shRNA was transfected with a construct expressing the full-length *KIF3A* cDNA (pCMV3-C-GFPSpark; Sino Biological, Bejing, China) using FuGENE HD (Promega) transfection reagent at 72 h after transduction. Rescue of cell migration defects was assessed at 48 h posttransfection. A Nikon A1Rsi inverted laser scanning confocal microscope, equipped with a motorized *x-y* stage, Tokai Hit microplate incubator and Perfect Focus System, was used to document cell migration. Cells were imaged at preselected *x-y* coordinate points in each well, once every 10 min during a period of 16–22 h. Cells were harvested and mRNA was isolated using a Qiagen RNeasy micro kit for quantitative RT-PCR (qRT-PCR) analysis. Cell migration was analyzed using a spot-tracking algorithm on Imaris software (Bitplane).

Flow cytometric analysis of lung cells

For flow cytometric analysis, total lung cell suspensions were prepared as previously described (37) from *A. fumigatus* extract–treated mice injected with brefeldin A 16 h prior to sacrifice. Lung tissues were enzymatically digested using caseinolytic units of Dispase (Discovery Labware; Corning) to obtain single-cell suspensions and stained using fluorochrome-labeled Abs. The gating strategies used are described in Rajavelu et al. (38). Eosinophils in lung cell suspensions were detected using Siglec-F PE (E50-2440; BD Pharmingen) and CCR3 FITC (J073E5; BioLegend) positive cells in the CD45 leukocyte gate. For analysis of ILC2 cells, the lineage mixture CD3/Ly-6G (Ly-6C)/CD11b/CD45R/Ter-119 Alexa Fluor 700 (79923; BioLegend), IL-7Rα FITC (A7R34; BioLegend), FLT3 allophycocyanin (A2F10; BioLegend), ST2 (DIH9; BioLegend), IL-17RB (752101; R&D Systems), and ICOS Pacific Blue (C398.4A; BioLegend) were used. T cells were analyzed using CD45 Alexa Fluor 700 (30-F11; BioLegend) and CD3ε FITC (145-2C11; BioLegend). For intracellular cytokine detection, mice were i.p. injected with brefeldin A (Sigma-Aldrich) and lung lobes were processed for single-cell suspensions as mentioned above followed by surface staining, then permeabilized with Cytofix/Cytoperm solution (BD Pharmingen) and stained for IL-4 PE/Cy7 (11B11; BioLegend) and IL-17A PerCP/Cy5.5 (TC11-18H10.1; BioLegend). The stained lung cell samples were acquired and analyzed on a Becton Dickinson FACSCanto III flow cytometer using FACSDiva software.

In vivo capillary–epithelial permeability

Experiments were performed as described by Davidovich et al. (39). In brief, 24 h after i.t. exposure to *Aspergillus* extract (100 μg) or saline, mice were anesthetized by isoflurane, and 0.3 ml of a 12 mg/ml solution of FITC-conjugated albumin (A9771; Sigma-Aldrich) was injected via tail vein. At the end of 3 h, blood was collected via direct cardiac puncture, and BAL was performed with 3 ml of normal saline. Albumin fluorescence in BALF and serum was determined using BioTek Synergy (BioTek Instruments, Winooski, VT) with absorption/emission wavelengths of 480/520 nm. Epithelial permeability was defined as the ratio of BALF to serum fluorescence.

Statistical analysis

Values are expressed as the mean ± SEM. Statistical analysis was performed using GraphPad Prism 6 software (GraphPad Software, La Jolla, CA). Data were analyzed using a two-tailed, unpaired Student *t* test or two-way ANOVA, and a Bonferroni correction was used for multiple comparisons. A p value ≤ 0.05 was considered statistically significant.

Results

Kif3a mRNA is widely expressed in many organs and tissue types and is widely expressed during fetal and postnatal lung development (40). In the developing mouse lung, *Kif3a* is expressed in multiple cell types, including cells of epithelial and mesenchymal origin. Because KIF3A is required for formation and function of both motile and primary cilia, we assessed the immunofluorescence staining of ARL13B and TUBB4A (β-tubulin IV) during perinatal and postnatal lung development in the mouse. Primary cilia were detected in both mesenchymal and epithelial cells in the fetal lung at embryonic day (E) 13.5 and E16.5 as identified by expression of ARL13B and lack of TUBB4A (Figs. 1A, 2A), whereas by E18.5 and postnatally, motile cilia coexpressing both proteins were readily detectable (Fig. 1B, 1C). The presence of abundant motile cilia in conducting airways made impossible the detection of potential primary cilia in multiciliated cells after E16.5 (Fig. 1C) (41). Primary cilia were not detected in club cells in the normal postnatal lung, consistent with previous findings (41).

We used mice bearing *Scgb1a1-Cre* or *Shh-Cre* to selectively delete exon 2 of the *Kif3a* gene. *Scgb1a1-Cre* is expressed early during the differentiation of conducting airway epithelial cells (around E16–17). As indicated by expression of enhanced GFP in Rosa Tomato (Red/Green) reporter mice, *Scgb1a1-Cre* caused extensive recombination in both ciliated and nonciliated airway epithelial cells at 8 wk of age (Fig. 1D); recombination was not observed in alveolar regions. Using this driver, the homozygous gene-deleted $Kif3a^{fl/fl}$;*Scgb1a1-Cre*$^+$ ($Kif3a^{Scg\Delta/\Delta}$) mice and heterozygous $Kif3a^{fl/+}$;*Scgb1a1-Cre*$^+$ ($Kif3a^{Scg\Delta/+}$) mice were generated. Controls were either $Kif3a^{fl/fl}$ or $Kif3a^{+/+}$;*Scgb1a1-Cre*$^+$ ($Kif3a^{Scg+/+}$). *Shh-Cre* is expressed throughout the developing lung epithelium beginning as early as E9.5 (42), resulting in targeting of the $Kif3a^{fl}$ alleles in most airway epithelial progenitor cells in proximal and peripheral conducting airways and in the alveoli, henceforth termed $Kif3a^{Shh\Delta/\Delta}$ and $Kif3a^{Shh\Delta/+}$ and the corresponding controls $Kif3a^{fl/fl}$ or $Kif3a^{Shh+/+}$. Both $Kif3a^{Scg\Delta/\Delta}$ and $Kif3a^{Shh\Delta/\Delta}$ mice were viable and present in normal Mendelian ratios after birth. The number and distribution of club, goblet, and cells staining for FOXJ1, a transcription factor selectively expressed in ciliated cells, were similar in $Kif3a^{fl/fl}$, $Kif3a^{Scg\Delta/+}$ and $Kif3a^{Scg\Delta/\Delta}$, and $Kif3a^{Shh\Delta/\Delta}$ mice (Figs. 1E, 1F, 2C, 2D). qRT-PCR demonstrated that *Foxj1* mRNA levels were unchanged, whereas *Arl13b* was significantly decreased in adult mice (Fig. 1G, 1H). A marked decrease in staining of acetylated α-tubulin (TUBA1A) was observed in $Kif3a^{Scg\Delta/\Delta}$ and $Kif3a^{Shh\Delta/\Delta}$ mice whereas expression of SCGB1A1 persisted in the club cells (Figs. 1E, 1F, 2C, 2D and data not shown). As an indication of the loss of KIF3A, the presence of primary cilia was evaluated in $Kif3a^{Shh\Delta/\Delta}$ mice. ARL13B staining revealed a dramatic reduction in the number of primary cilia in the developing lung epithelial cells, whereas no changes were detected in the adjacent mesenchyme (Fig. 2A, 2B). Cells disassociated from adult whole lungs isolated from $Kif3a^{Shh\Delta/\Delta}$ and $Kif3a^{Shh+/+}$ mice were sorted using the epithelial marker EpCAM. Exon 2–specific primers were used to demonstrate a reduction in *Kif3a* mRNA in $Kif3a^{Shh\Delta/\Delta}$ cells (Fig. 2E, 2F). Consistent with the reduction of acetylated tubulin staining, numbers, size, and shape of motile cilia were reduced in $Kif3a^{Shh\Delta/+}$ and $Kif3a^{Shh\Delta/\Delta}$ mice by scanning electron microscopy (Fig. 2G–I). Abnormalities in cilia were most prominent in the homozygous $Kif3a^{Shh\Delta/\Delta}$ mice. To assess mucociliary clearance after deletion of *Kif3a*, video imaging of tracheal and large airway fluid dynamics and ciliary activity were measured in $Kif3a^{Shh\Delta/\Delta}$, $Kif3a^{Scg\Delta/\Delta}$, and control mice. Consistent with the extensive loss of motile cilia from the airway epithelium, ciliary beat frequencies were markedly decreased in airways of both

Downloaded from http://www.jimmunol.org/ at Liverpool University Library on December 12, 2016

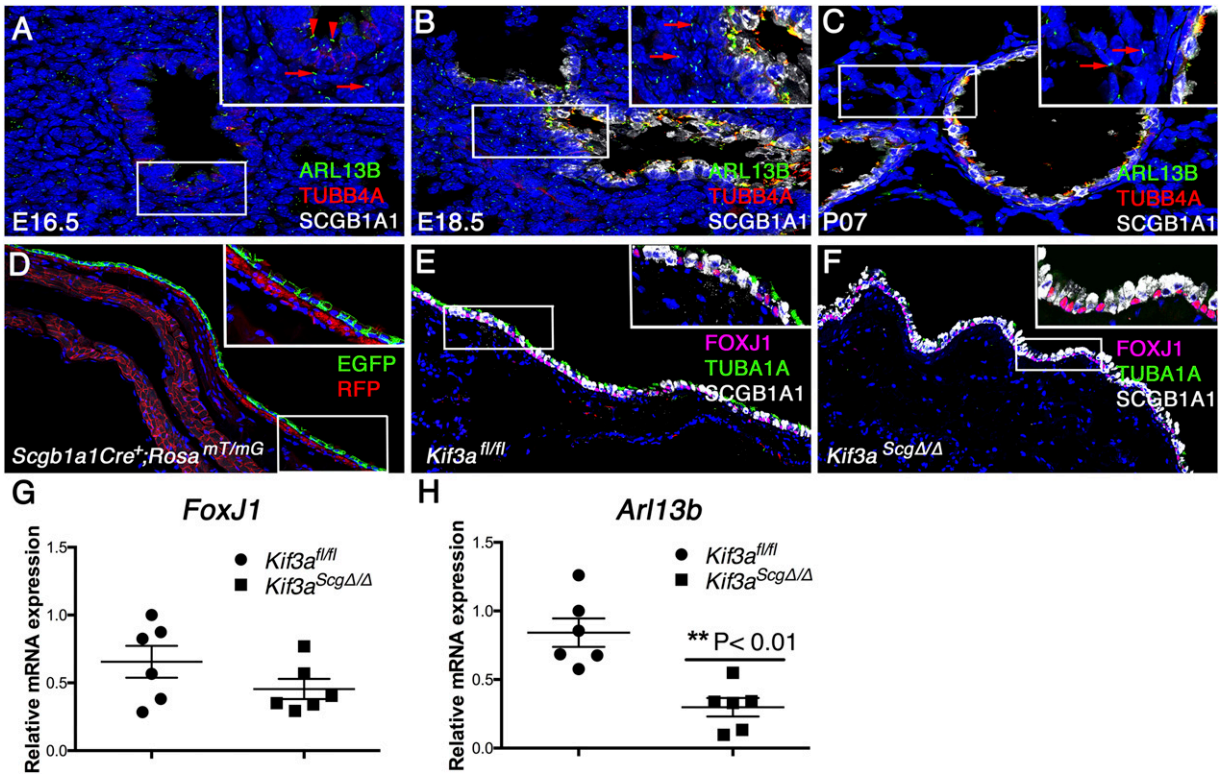

FIGURE 1. Conditional deletion of *Kif3a* in the airway epithelium. At E16.5, primary cilia are detected by ARL13B staining in the fetal lung epithelium and mesenchyme (red arrows) and absence of TUBB4A (**A**). At E18.5 (**B**) and postnatal day 7 (P07) (**C**), the presence of motile cilia (staining for ARL13B and TUBB4A) obscures detection of primary cilium. ARL13B staining was not detected in SCGB1A1-stained club cells (original magnification ×60). Enhanced GFP in Rosa Tomato (Red/Green) reporter mice (**D**) was used to assess the extent of recombination by *Scgb1a1-Cre* at 8 wk of age. Cilia were stained for TUBA1A (green) in $Kif3a^{fl/fl}$ control mice (**E**). Cilia were lacking after deletion of *Kif3a* in $Kif3a^{Scg\Delta/\Delta}$ mice (**F**) (D–F) Original magnification ×20. FOXJ1 staining was unchanged (red, E and F). The number and distribution of club cells staining with SCGB1A1 (white) were not altered in $Kif3a^{Scg\Delta/\Delta}$ airways. qRT-PCR on whole-lung cDNA from adult mice (**G** and **H**) ($n = 6$ per genotype) demonstrated decreased *Arl13b* mRNA (**$p < 0.01$ by *t* test compared with controls), consistent with loss of *Kif3a*.

$Kif3a^{Shh\Delta/+}$ and $Kif3a^{Shh\Delta/\Delta}$ mice and fluorescent bead movement lost directionality (Fig. 2J, 2K, Supplemental Videos 1, 2). Taken together, these observations indicate that primary cilia are not required for cell fate specification of the airway epithelial cells and that deletion of *Kif3a* by either *Shh-Cre* or *Scgb1a1-Cre* (data not shown) inhibits ciliary function and inhibits mucociliary clearance.

Enhanced Th2 inflammation and AHR in Kif3a *gene–targeted mice after aeroallergen exposure*

To assess the role of *Kif3a* during aeroallergen sensitization, adult $Kif3a^{Scg+/+}$, $Kif3a^{fl/fl}$, $Kif3a^{Scg\Delta/+}$, and $Kif3a^{Scg\Delta/\Delta}$ mice were repeatedly treated with relatively low concentrations of *A. fumigatus* or HDM extract. At baseline, under our pathogen-free vivarium conditions, no histological evidence of pulmonary inflammation was observed in $Kif3a^{Scg\Delta/\Delta}$ and $Kif3a^{Scg\Delta/+}$ mice, nor were there differences in AHR or inflammatory responses following exposure to saline (Fig. 3). Following i.t. *A. fumigatus* extract sensitization, similar AHR and inflammatory responses were observed in control $Kif3a^{fl/fl}$ and $Kif3a^{Scg+/+}$ mice. In contrast, AHR and the inflammatory responses were significantly increased in $Kif3a^{Scg\Delta/\Delta}$ and $Kif3a^{Scg\Delta/+}$ mice (Fig. 3). AHR was most increased in homozygous *Kif3a*-deleted mice (Fig. 3A). Numbers of inflammatory cells, consisting primarily of eosinophils, were increased in the BALF from both $Kif3a^{Scg\Delta/+}$ and $Kif3a^{Scg\Delta/\Delta}$ mice after aeroallergen challenge (Fig. 3B, 3C). We observed no differences in plasma levels of *Aspergillus*-specific IgG1 in the exposed mice of each genotype (Supplemental Fig. 1A). Goblet cell metaplasia and mucus hyperproduction were observed in mice of all *Kif3a* genotypes after exposure to *A. fumigatus* extract and were more severe in the $Kif3a^{Scg\Delta/\Delta}$ and $Kif3a^{Scg\Delta/+}$ mice (Fig. 3D–F, Supplemental Fig. 1B). Consistent with these findings, AHR was significantly increased in *Kif3a* gene–deleted mice after HDM exposure (Supplemental Fig. 2).

The increased inflammatory responses to *A. fumigatus* extract observed in the *Kif3a*-deleted mice were supported by mRNA expression data (Table I). Histological and immunofluorescence studies demonstrating increased goblet cell metaplasia after exposure to *Aspergillus* extract were supported by increased expression of *Spdef*, *Foxa3*, *Clca1*, and *Muc5b* mRNAs in lungs from $Kif3a^{Scg\Delta/\Delta}$ mice. Likewise, *Il-13*, *Il-4*, *Il-17a*, *Ccl11*, and *Ear11* mRNAs were significantly increased in lungs of both $Kif3a^{Scg\Delta/\Delta}$ and $Kif3a^{Scg\Delta/+}$ mice, indicating Th2-mediated eosinophilic inflammation (Fig. 3D–F, Table I). We used flow analysis to identify the inflammatory cells present following *Aspergillus* extract administration to $Kif3a^{Scg\Delta/\Delta}$ mice. Numbers of Siglec-F^+/$CCR3^+$ cells in whole-lung digests were increased in lungs of $Kif3a^{Scg\Delta/\Delta}$ mice, consistent with the increased eosinophils seen in the BALF; likewise, IL-4^+ and IL-$17A^+$ T cells were increased, consistent with enhanced Th2 and Th17 responses in *Kif3a* gene–deleted mice (Fig. 4).

Similar to *Kif3a*, *Ift88* is a microtubule-associated transport protein required for both primary and motile cilia formation in airway epithelial cells (43, 44). The *Scgb1a1-Cre* and *Shh-Cre* transgenes were bred into the $Ift88^{fl/fl}$ animals to create *Ift88* gene–deleted lung epithelium. At baseline, histological findings in the $Ift88^{Scg\Delta/\Delta}$ and $Ift88^{Shh\Delta/\Delta}$

Downloaded from http://www.jimmunol.org/ at Liverpool University Library on December 12, 2016

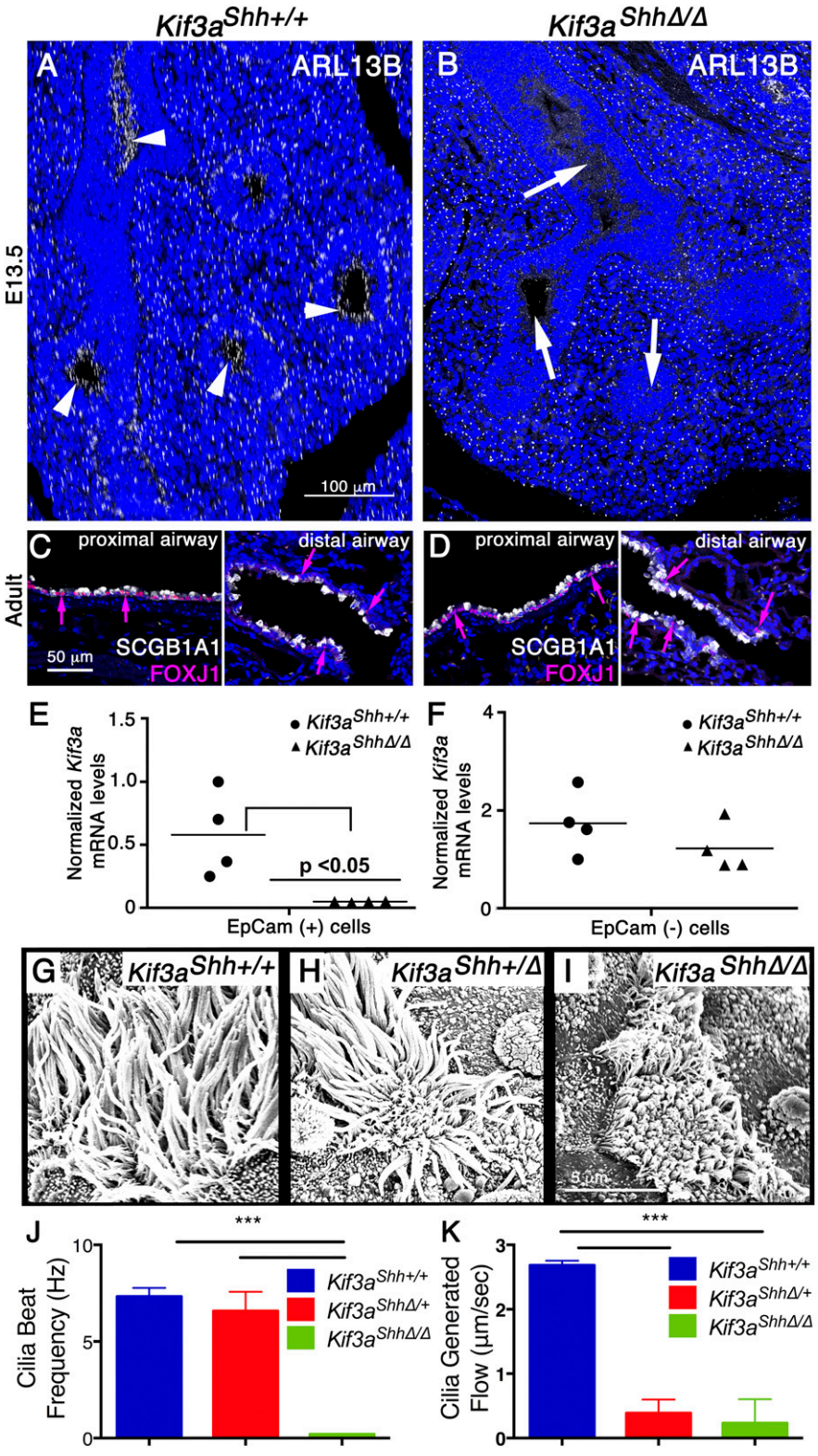

FIGURE 2. Loss of primary cilia, ciliary beating, and mucociliary clearance in *Kif3a*$^{Shh\Delta/\Delta}$ mice. *Kif3a* was deleted under control of *Shh-Cre*. At E13, primary cilia, identified by ARL13B staining, were absent in *Kif3a*$^{Shh\Delta/\Delta}$ airway epithelial cells (**B**, arrows), compared with *Kif3a*$^{Shh+/+}$ embryos (**A**, arrowheads). Figures are representative of $n = 3$ per genotype (tile scans, original magnification ×60). Staining of ciliated (FOXJ1^{+} nuclei, pink arrows) and club (SCGB1A1, white) cells is shown in the bronchiolar epithelial cells in adult airways (**C** and **D**) ($n = 4$ per genotype); (original magnification ×60). *Kif3a* mRNA levels were evaluated using exon 2–specific primers. A decrease in *Kif3a* mRNA was detected in EpCAM^{+}- but not EpCAM^{-}-sorted cells from adult *Kif3a*$^{Shh\Delta/\Delta}$ mice ($n = 4$ per genotype, $p < 0.05$ by t test) (**E** and **F**). Motile cilia were identified in control, *Kif3a*$^{Shh+/\Delta}$, and *Kif3a*$^{Shh\Delta/\Delta}$ airways by scanning electron microscopy (**G–I**); (original magnification ×5000). Uniformly short cilia were observed in *Kif3a*$^{Shh\Delta/\Delta}$ airways ($n = 3$ per genotype). Tracheas of adult mice were excised, perfused, and differential interference contrast images viewed longitudinally after introduction of fluorescent microspheres (0.20 μm). Movements of individual beads were followed by video microscopy. Cilia beat frequency was quantified (**J**). Cilia-generated flow was imaged by tracking the fluorescent microspheres (**K**). Data represent the mean ± SEM of $n = 3$ mice per group. ***$p < 0.001$ by one-way ANOVA.

mice were similar to those seen after epithelial deletion of *Kif3a* in which specification of lung epithelial cells and absence of motile cilia were observed (Fig. 5A–D and data not shown). *Ift88*$^{fl/fl}$ and *Ift88*$^{Scg\Delta/\Delta}$ were exposed to *A. fumigatus* or saline using the same sensitization protocol used with the *Kif3a* gene–targeted mice. Pulmonary eosinophilic inflammation and Alcian blue staining of airway cells were similar in *Ift88*$^{Scg\Delta/\Delta}$ and controls after exposure to *Aspergillus* extract (Fig. 5E–H). Although an increase in mRNAs associated with goblet cells was observed in *Ift88*$^{Scg\Delta/\Delta}$ mice after exposure, neither *Ear11* nor Th2-related cytokine mRNAs were increased to the levels seen in the *Kif3a*-deleted mice (Table I). AHR was not evaluated in these animals because *Ift88*$^{Shh\Delta/\Delta}$ mice were found to have hyperreactive airways at baseline (43). Taken together, both *Kif3a*$^{Scg\Delta/+}$ and *Kif3a*$^{Scg\Delta/\Delta}$ mice were more susceptible to Th2-mediated eosinophilic pulmonary inflammation than were the *Ift88*$^{Scg\Delta/\Delta}$

Downloaded from http://www.jimmunol.org/ at Liverpool University Library on December 12, 2016

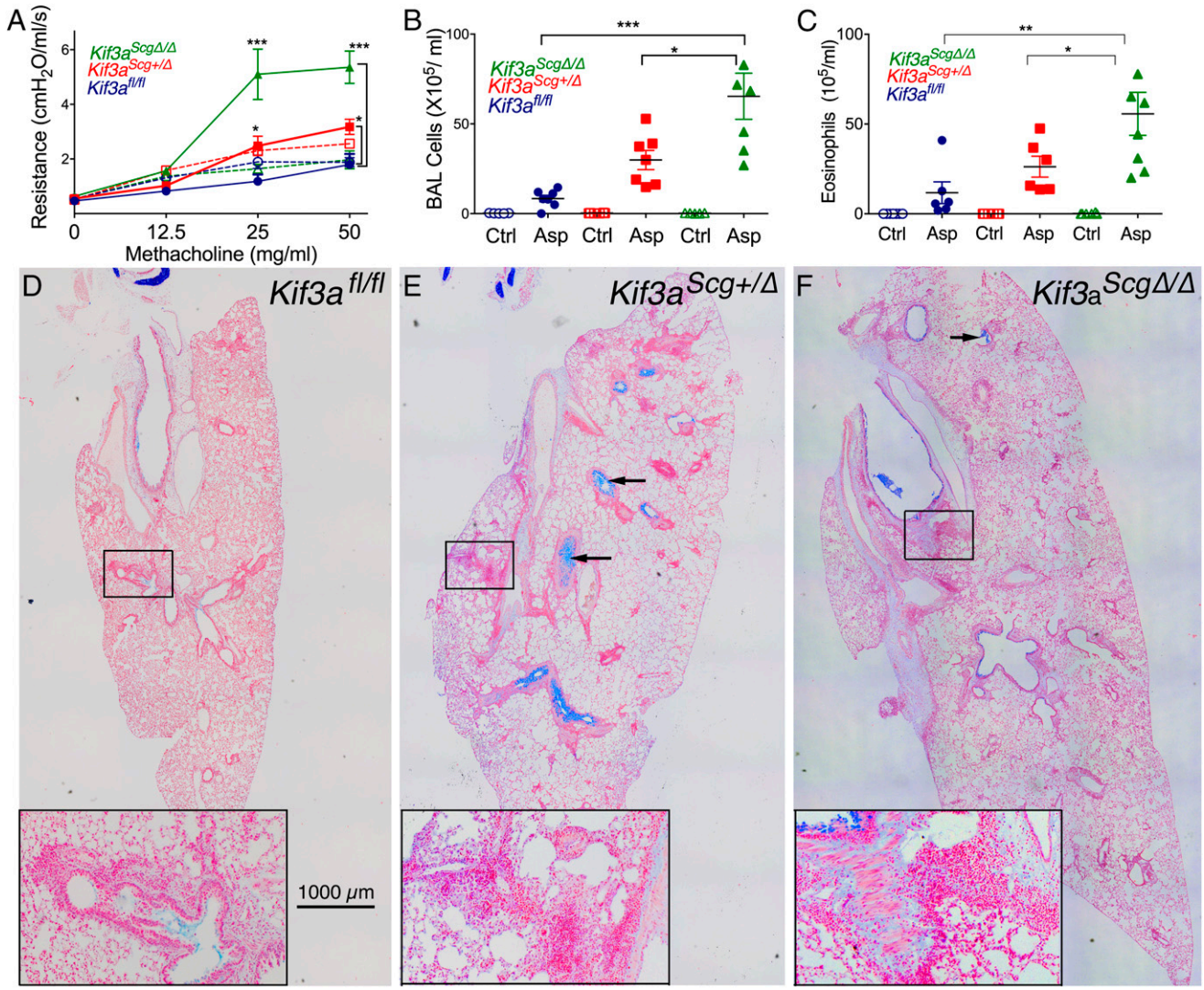

FIGURE 3. Increased AHR and eosinophilic inflammation in *Kif3a* gene–deleted mice. Age-matched mice were sensitized with *A. fumigatus* Ag or saline. AHR is represented as resistance in response to methacholine. *Aspergillus*-treated mice are represented as solid lines and saline-treated mice as dashed lines (**A**). Total number of cells in BALF was determined (**B**). Eosinophil numbers were calculated (**C**). Data represent the mean ± SEM of six to seven mice per group. *$p < 0.05$, **$p < 0.01$, ***$p < 0.001$ by two-way ANOVA. Increased inflammation and mucus were present in both *Kif3a* gene deletants shown by representative (original magnification ×4) tile scans after Alcian blue and nuclear fast red staining (**D**–**F**).

mice, indicating a distinct role for *Kif3a* in asthma-like pulmonary inflammation.

KIF3A is required for epithelial repair

Because primary cilia play important roles in the regulation of proliferation, migration, and differentiation, we assessed airway epithelial repair by treating adult mice with naphthalene. Naphthalene is metabolized to a cellular toxicant by CYP2F2, a p450 enzyme that is selectively expressed in most nonciliated conducting airway cells in the mouse lung (45, 46). CYP2F2 was normally expressed by club cells in *Kif3a*-deficient airways. After naphthalene exposure, resistant progenitor cells rapidly migrate, proliferate, and differentiate to repair the airways. Seven days after naphthalene exposure, areas of damaged airway were present in both the control and *Kif3a* gene–deleted airways (Fig. 6A, 6B). In control mice, the distribution of both ciliated and epithelial club cells was restored 10 d after naphthalene injection (Fig. 6C, 6E, 6G). Repair of the airway epithelium in $Kif3a^{Scg\Delta/\Delta}$ mice was incomplete, as indicated by significantly decreased numbers of club cells and squamous cell metaplasia (Fig. 6D, 6F, 6G), demonstrating that KIF3A was required for normal repair of the conducting airway epithelium.

KIF3A mediates epithelial cell migration

To assess the role of KIF3A in cell proliferation and migration, *KIF3A* mRNA was inhibited in human bronchial epithelial cells (HBEC3) and BEAS-2B cells with lentiviral shRNA, and cell migration was assessed by video imaging. When *KIF3A* mRNA was selectively inhibited, cells adhered to the plates, proliferated, and reached confluency at 72 h posttransduction. Primary cilia were identified by costaining of ARL13B and acetylated α-tubulin (ac-TUBA4A) in BEAS-2B cells (Fig. 7C). Motile cilia were not detected in these cell lines. Inhibition of *KIF3A* was confirmed by qRT-PCR, whereas expression of a nontargeted gene, *CDH1*, was unchanged (Fig. 7D). *KIF3A* knockdown suppressed formation of primary cilia and markedly inhibited cell movement and migration in "scratch" assays (Fig. 7A, 7B; see Supplemental Videos 3, 4). *KIF3A* shRNA did not alter proliferation of HBEC3 cells (Fig. 7E); however, phospho–histone H3 staining was modestly decreased by *KIF3A* knockdown in BEAS-2B cells at confluency (data not shown). Cytoplasmic staining of ac-TUBA4A was altered by inhibition of *Kif3a*, indicating a potential role of KIF3A in microtubule assembly (Supplemental Fig. 3A). Cell

Downloaded from http://www.jimmunol.org/ at Liverpool University Library on December 12, 2016

Table I. Increased expression of RNAs related to Th2 inflammation and goblet cell differentiation

Gene	TaqMan Probe ID	Fold Increase Relative to Controls (Mean ± SEM)		
		Kif3a$^{ScgΔ/+}$	*Kif3a*$^{ScgΔ/Δ}$	*Ift88*$^{ScgΔ/Δ}$
Acta2	Mm00725412_s1	1.7 ± 0.6	3.3 ± 1.2	5.5 ± 3.4
Ccl11	Mm00441238_m1	36.4 ± 21.1[a]	171.1 ± 144.1[a]	0.3 ± 0.1
Ccl17	Mm00516136_m1	7.6 ± 2.8	21.3 ± 17.0	3.2 ± 1.1
Ccl2	Mm00441242_m1	5.5 ± 3.2	2.3 ± 1.0	0.7 ± 0.3
Ccl24	Mm00444701_m1	15.5 ± 9.1	6.0 ± 3.0	2.5 ± 1.1
Cdh1	Mm00480906_m1	1.1 ± 0.3	1.5 ± 0.3	1.3 ± 0.3
Clca1	Mm00777368_m1	2.4 ± 0.6	14.4 ± 11.2[b]	2.5 ± 0.9
Csf2	Mm01290062_m1	1.2 ± 0.5	2.5 ± 1.2	4.9 ± 2.2
Cxcl1	Mm04207460_m1	1.6 ± 0.7	4.1 ± 1.9	5.0 ± 2.4
Ear11	Mm00519056_s1	18.4 ± 8.0[b]	26.7 ± 6.5[b]	4.7 ± 2.7
Foxa3	Mm00484714_m1	2.5 ± 0.5	18.7 ± 14.3[b]	11.4 ± 4[b]
Ifnγ	Mm01168134_m1	3.8 ± 0.6	3.3 ± 1.09	5.3 ± 2.5
Il4	Mm00445259_m1	6.7 ± 1.4[b]	29.6 ± 21.7[b]	1.8 ± 0.4
Il13	Mm00434204_m1	8.9 ± 2.6[b]	25.4 ± 11.4[b]	1.9 ± 0.5
Il17A	Mm00439618_m1	78.7 ± 52.6[c]	10.3 ± 3.4[d]	3.5 ± 1.2
Il33	Mm00434204_m1	2.3 ± 0.6	3.3 ± 0.9	2.1 ± 1.1
Il5	Mm00439646_m1	3.4 ± 0.6	9.5 ± 6.6	2.2 ± 0.7
Il6	Mm00446190_m1	4.4 ± 2.7	2.7 ± 0.7	3.8 ± 1.2
Muc5ac	Mm01276725_g1	4.1 ± 2.1	8.5 ± 5.6	3.1 ± 1.8
Muc5b	Mm00466391_m1	5.3 ± 2.8	6.1 ± 2.1[b]	6.8 ± 2.9[b]
Spdef	Mm00600221_m1	4.7 ± 1.1[b]	10.8 ± 5.9[b]	7.2 ± 3.7[b]
Tslp	Mm01157588_m1	2.1 ± 0.8	2.2 ± 0.9	4.3 ± 2.2

qRT-PCR was performed on whole-tissue RNA collected from the right lungs of mice sensitized with *Aspergillus* extract. Fold change in mRNA levels of *Kif3a*$^{ScgΔ/+}$ and *Kif3a*$^{ScgΔ/Δ}$ compared with *Kif3a*$^{fl/fl}$ and *Ift88* gene deletants compared with *Ift88*$^{fl/fl}$ control mice is shown after normalization to 18S. Age-matched mice (n = 6–7 per group) are shown. *Il17A* RNA was barely detectable at baseline and was readily detected in both *Kif3a* deletants.

[a] $p < 0.01$ by one-way ANOVA followed by a Bonferroni multiple comparison test.

[b] $p < 0.05$.

[c] $p = 0.024$ by ANOVA on ranks.

[d] $p = 0.0388$ by two-tailed t test.

tracking analysis showed that inhibition of KIF3A did not cause cell death but inhibited cell movement and migration trajectory characteristics; for example, displacement, directionality, speed, and persistence. Expression of the human *KIF3A* cDNA substantially rescued cell motility and navigation (Supplemental Fig. 3B). Loss of KIF3A was associated with dramatic inhibition of cell movement and disruption of cytoplasmic microtubule organization, indicating its important role in bronchial epithelial cell migration, findings consistent

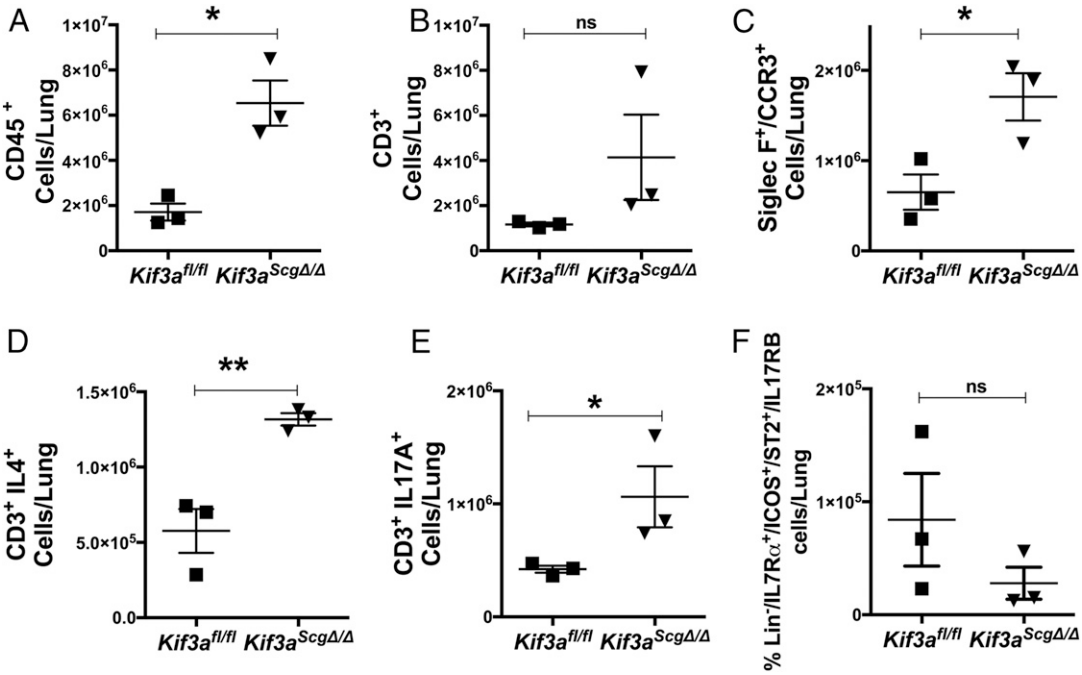

FIGURE 4. Deletion of *Kif3a* in airway epithelial cells increased recruitment of IL-4$^+$ and IL-17$^+$ T cells. Flow cytometric analysis of lung cells from *Kif3a*$^{fl/fl}$ (■) and *Kif3a*$^{ScgΔ/Δ}$ (▼) mice after i.t. administration of *A. fumigatus* extract (10 μg, nine times during a 2-wk period). Numbers of CD45$^+$ leukocytes (**A**) and CD3$^+$ T cells (**B**) are shown. Eosinophilic inflammation was assessed by Siglec-F$^+$/CCR3$^+$ cells (**C**). Numbers of IL-4$^+$ and IL-17$^+$ CD3$^+$ T cells (**D** and **E**) were significantly increased in *Kif3a*$^{ScgΔ/Δ}$ mice. ILC2 (Lin$^-$/IL-7Rα$^+$/ICOS$^+$/ST2$^+$/IL-17RB$^+$) cell numbers in *Kif3a*$^{fl/fl}$ and *Kif3a*$^{ScgΔ/Δ}$ mice were unaltered (**F**). Graphs represent mean ± SEM. *$p < 0.05$, **$p < 0.005$, compared with controls using one-way ANOVA (n = 3 animals per genotype). ns, not significant.

Downloaded from http://www.jimmunol.org/ at Liverpool University Library on December 12, 2016

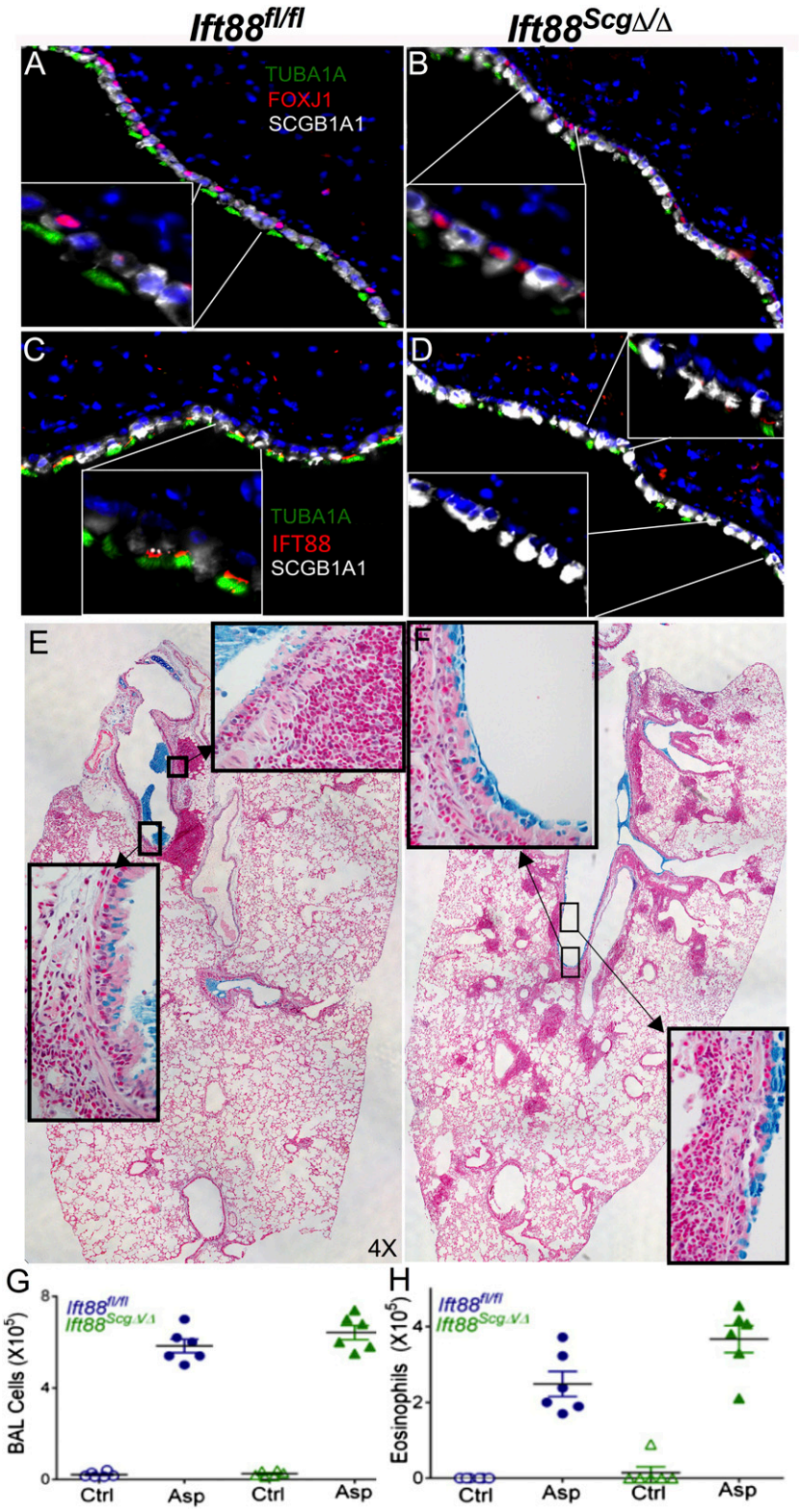

FIGURE 5. Response to *Aspergillus* sensitization in $Ift88^{Scg\Delta/\Delta}$ mice. Acetylated TUBA1A (green)–stained cilia in $Ift88^{fl/fl}$ controls (**A**) were nearly absent in $Ift88^{Scg\Delta/\Delta}$ mice (**B**). FOXJ1, a transcription factor expressed in ciliated cells, was unchanged (B). The number and distribution of club cells staining for SCGB1A1 (white) were not altered in $Ift88^{Scg\Delta/\Delta}$ airways (A–**D**) (original magnification ×20). IFT88 staining (green) was nearly absent in $Ift88^{Scg\Delta/\Delta}$ mice (C versus D). Age-matched mice (6–8 wk at initial sensitization) were sensitized three times per week for 3 wk with 10 μg of *A. fumigatus* Ag or saline i.t. (n = 6–7 mice per genotype). Alcian blue and nuclear red staining of whole left lobes was unchanged (**E** and **F**); tile scans, original magnification ×4. The number of cells in BALF was not altered (**G**). Eosinophil numbers were calculated from total numbers of BALF cells, and differential cell counts and were not statistically different (**H**) as determined by one-way ANOVA.

with the failure of airway epithelial repair seen after naphthalene-induced injury in the $Kif3a^{Scg\Delta/\Delta}$ mice in vivo.

Increased capillary epithelial permeability in $Kif3a^{Shh\Delta/\Delta}$ mice

Because loss of barrier function is associated with asthma-like pathology and Th2 inflammation (47), we tested whether capillary–epithelial permeability was altered in the $Kif3a^{Shh\Delta/\Delta}$ mice in vivo. Twenty-four hours after exposure to one dose of *Asperillus* extract (i.t.), mice were injected with fluorescein-congugated albumin via tail vein followed by quantification of fluorescein in BALF and serum. Capillary–alveolar permeability was significantly increased in the *Kif3a* gene–deleted mice (Fig. 6H).

Discussion

The present findings demonstrate the important role of airway epithelial KIF3A in the pathogenesis of aeroallergen-induced inflammation and AHR, linking the activities of microtubules

Downloaded from http://www.jimmunol.org/ at Liverpool University Library on December 12, 2016

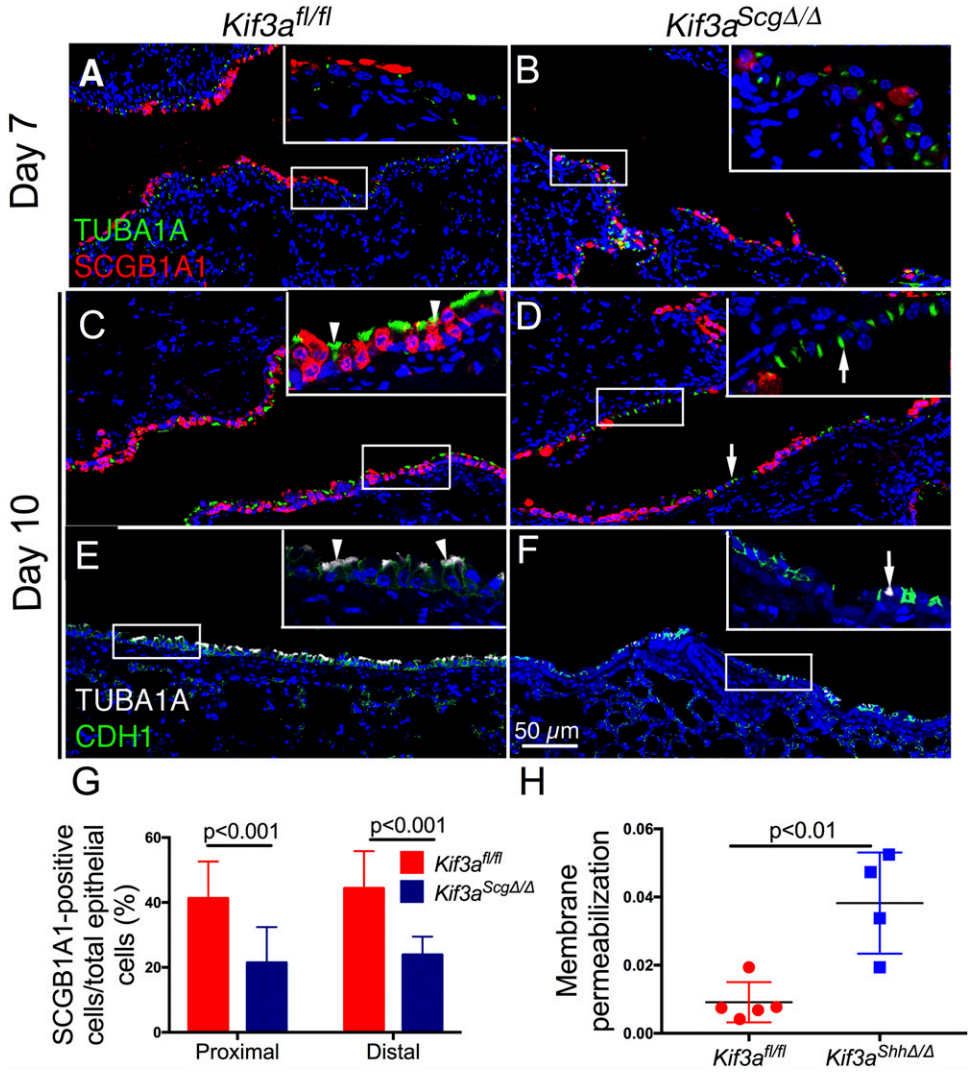

FIGURE 6. *KIF3A* is required for repair of the airway epithelium. Mice of each genotype were injected i.p. with one dose of naphthalene. Mice were sacrificed on day 7 ($n = 3$) (**A** and **B**) and on day 10 ($n = 4$) (**C**–**F**). Lung sections were immunostained for SCGB1A1 (red) and acetylated TUBA1A [green in (A)–(D)]. In (E) and (F), CDH1 (E-cadherin) is shown in green and TUBA1A in white. Restoration of bronchial epithelial cells is shown in controls, and persistence of squamous metaplasia and paucity of SCGB1A1-stained cells is shown in the $Kif3a^{Scg\Delta/\Delta}$ mice. For quantitation of regenerated cells, magnified images (original magnification ×20) of comparable regions (five proximal and five distal regions) from control and mutant mice were evaluated (**G**) using ImageJ software with plugin-Fiji). The percentage of regenerated cells was calculated by counting SCGB1A1-stained cells and the total number of DAPI-stained epithelial nuclei. The number of club cells was significantly decreased in $Kif3a^{Scg\Delta/\Delta}$ mice on day 10 (G). (**H**) Increased capillary–epithelial permeability in $Kif3a^{Shh\Delta/\Delta}$ mice. FITC-labeled albumin was injected into the tail vein of four to five adult mice of each genotype 24 h after i.t. treatment with one dose of *Aspergillus* extract (100 μg). The concentration of the FITC label in the serum and BALF was measured by 3 h after injection and the ratio was calculated. $***p < 0.001$ by t test.

to innate immune responses to aeroallergens. Enhanced AHR, goblet cell–associated gene expression, and Th2-mediated eosinophilic inflammation observed after deletion of *Kif3a* provide a plausible mechanistic link between the genetic association of *KIF3A* alleles, levels of KIF3A protein, microtubule function, and asthma (15, 16). Although complete deletion of *Kif3a* is lethal in embryonic development (20–22), present studies demonstrate that loss of *Kif3a* in airway epithelial cells impairs mucociliary clearance, epithelial repair following injury, and enhances Th2 inflammation that together may influence responses to aeroallergens. *A. fumigatus* infection causes allergic bronchopulmonary aspergillosis associated with individuals with asthma, cystic fibrosis, and primary ciliary dyskinesia; patients with allergic bronchopulmonary aspergillosis are also at risk for eczema, hives, hay fever, and sinusitis (48, 49).

Increased AHR was seen in $Kif3a^{Scg\Delta/+}$ and $Kif3a^{Scg\Delta/\Delta}$ mice following repeated exposures to *A. fumigatus* or HDM extract. A major *A. fumigatus* allergen, ASPF13, promotes AHR, recruiting inflammatory cells to the bronchial submucosa and disrupting airway smooth muscle cell–extracellular matrix interactions (50). AHR was assessed by plethysmography, a measure of both smooth muscle hyperplasia and contractility, and mucus hyperproduction. In the present studies, we did not detect differences in ACTA2 staining in bronchial smooth muscle, and *Acta2* mRNA was not significantly increased in the $Kif3a^{Scg\Delta/\Delta}$ mice after *Aspergillus* sensitization. Thus, mechanisms involved in the observed AHR are presently unclear. However, expression of *Il-13* and *Il-4* RNAs were markedly increased in both heterozygous and homozygous *Kif3a*-deleted mice after sensitization, with both factors being known to directly activate IL-4Rα receptor signaling in bronchial smooth muscle cells causing AHR (51). Increased secretion of chemokines and cytokines recruiting inflammatory cells, including eosinophils, has been associated with increased smooth muscle

Downloaded from http://www.jimmunol.org/ at Liverpool University Library on December 12, 2016

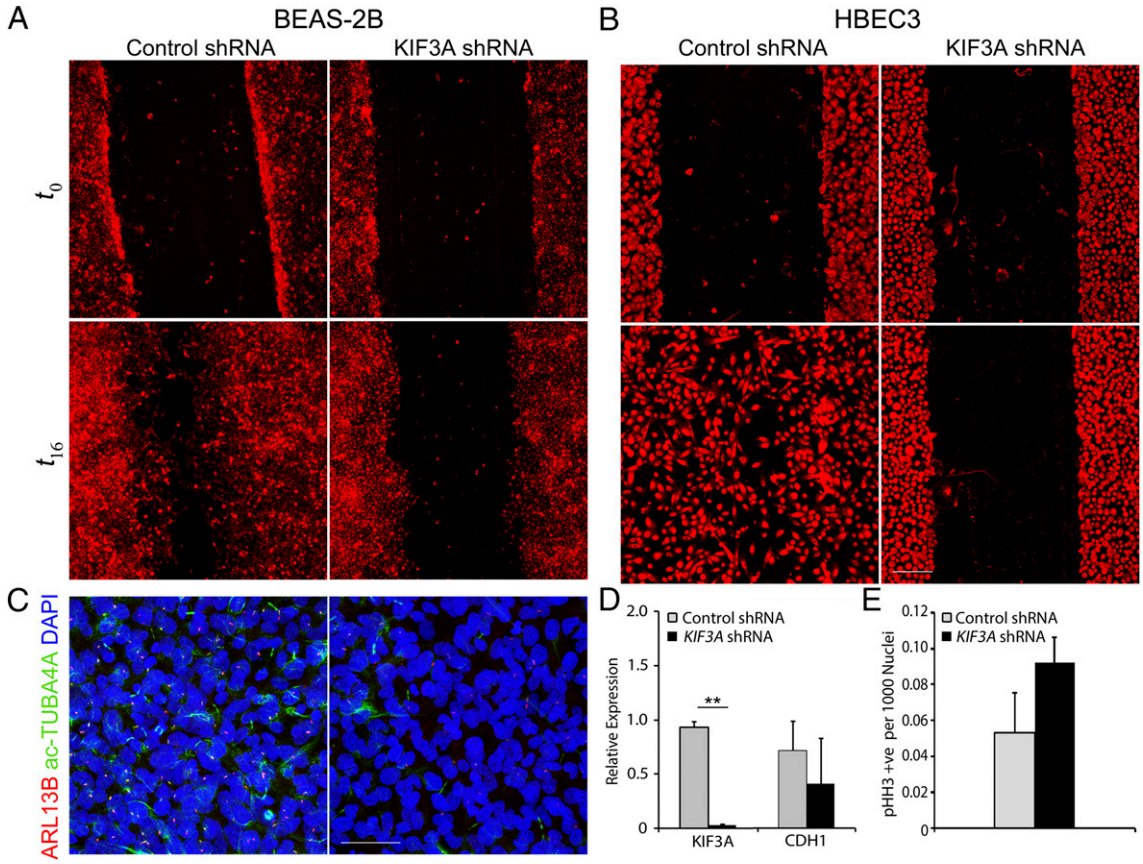

FIGURE 7. KIF3A is required for cell migration in vitro. HBEC3 and BEAS2B cells were transduced with control and KIF3A shRNA lentiviruses. Cells were stained with di-8-ANEPPS and the monolayer was wounded by mechanical scratch. *Kif3a* mRNA was decreased by the shRNAs (**D**) ($n = 4$). Inhibition of *Kif3a* inhibited cell migration was observed by videography for 16 h; data are representative of $n = 3$ independent experiments in BEAS2B (**A**) and HBEC3 (**B**). Costaining for ARL13B and ac-TUBA4A showed loss of primary cilia in BEAS-2B cells (**C**). ARL13B staining was not detected in HBEC3 cells (data not shown). Immunofluorescence data are representative of $n = 2$ independent experiments. (**E**) Average number of pHH3 nuclei detected per 1000 DAPI-stained nuclei. Proliferation was unaltered by knockdown of *Kif3a* in HBEC3 cells. Data represent mean ± SEM of nuclei from 6 to 10 images per group. (A and B) Original magnification ×10; (C) original magnification ×60.

cell activity in asthma (52). Accumulation of mucus in conducting airways seen in both *Kif3a*$^{Scg\Delta/\Delta}$ and *Kif3*$^{Scg\Delta/+}$ mice may also contribute to AHR.

The present studies demonstrate diverse functions of KIF3A in airway epithelial cells, including epithelial repair, innate immune responses, and mucociliary clearance, that may influence airway reactivity and Th2 inflammation. There is strong experimental evidence linking the loss of barrier function, epithelial injury, and mucociliary clearance in the pathogenesis of asthma (47, 53, 54). Patients with primary ciliary dyskinesia have recurrent airway infections related to poor mucociliary clearance (55, 56), and expression of cilia-related genes, including *KIF3A*, were decreased during acute asthma (57). Reduced mucociliary clearance and increased susceptibility to infection related to motile ciliary dysfunction were proposed to contribute to the pathogenesis of asthma (58). KIF3A is known to play important roles in microtubule assembly and intracellular transport of multiple protein cargos, in addition to its known role in the formation of primary and motile cilia (17–19). It is therefore likely that changes in KIF3A levels or function play diverse roles in respiratory epithelial cell homeostasis. *Aspergillus* and HDM extracts contain proteases, Ags, and other inflammatory mediators that cause epithelial cell injury (59, 60). Decreased mucociliary clearance, increased uptake of Ag by dendritic cells, and disrupted microtubular transport within the epithelial cells may influence the increased Th2 responses seen following deletion of *Kif3a*. Changes in barrier function may influence cytokine and chemokine signaling from the epithelium to regulate recruitment and activation of dendritic and ILC2 cells, in turn recruiting Th2 and Th17 cells mediating asthma-like pulmonary inflammation [(37); for review, see Fahy (61) and Lambrecht and Hammad (62)]. Increased *Il-13*, *Il-4*, *Ccl11*, *Il-17A*, and *Ccl24* RNAs seen in lungs of the *Kif3a*-deleted mice are consistent with the observed Th2-mediated inflammation. *Ccl11* (eotaxin1), a potent eosinophil chemoattractant, was markedly induced in the *Kif3a*- but not the *Ift88*-deleted mice. Increased expression of *Il-13* and *Il-4* seen after *Aspergillus* extract in the *Kif3a*$^{Scg\Delta/\Delta}$ mice is typical of canonical Th2 lymphocytic responses that influence goblet cell metaplasia and mucus hyperproduction (63). Likewise, increased levels of *Spdef*, *Foxa3*, *Muc5b*, and *Muc5ac* in the *Kif3a*$^{Scg\Delta/\Delta}$ mice are consistent with goblet cell metaplasia being related to the activation of Th2-induced IL-4R signaling and STAT6 activation that occur following aeroallergen exposure (38, 64, 65).

Repair of the respiratory epithelium was impaired and capillary–epithelial barrier function was decreased, factors that may contribute to the enhanced Th2 inflammation seen in the *Kif3a* gene–deleted mice. Primary cilia influence cell migration, a process critical for repair (66, 67). Decreased expression of KIF3A inhibited migration of both BEAS-2B and HBEC3 cells in vitro, findings consistent with impaired epithelial repair seen in *Kif3a*$^{Scg\Delta/\Delta}$ mice after exposure to naphthalene. These findings are supported by previous in vitro studies demonstrating the role of KIF3A in cell migration in kidney epithelial cells (27). Recent in vitro findings

Downloaded from http://www.jimmunol.org/ at Liverpool University Library on December 12, 2016

demonstrated that the disruption of microtubules seen after inhibition of *KIF3A* did not occur after inhibition of *IFT88* (68). Inflammatory responses to *Aspergillus* were increased in both *Ift88*- and *Kif3a*-deleted mice, although Th2 responses were more pronounced in the $Kif3a^{Scg\Delta/\Delta}$ mice, supporting the concept that the microtubule-associated proteins may have distinct as well as overlapping functions in innate immune regulation in the airway epithelial cells.

The present findings demonstrate that KIF3A was required for suppression of Th2-mediated inflammatory responses, mucus hyperproduction, and AHR following aeroallergen exposure, findings that support the association of *KIF3A* gene polymorphisms with clinical susceptibility to allergic asthma and rhinitis (11–16). Previous clinical findings in nasal epithelial cells demonstrated decreased expression of *KIF3A* during acute asthma exacerbations (57). Because in the present study, increased lung inflammation and AHR were observed in haploinsufficient mice, even a modest decrease in KIF3A expression may influence the susceptibility to Th2-mediated inflammation. Previous observations that the human *KIF3A* gene locus is located contiguously with the *IL-4/IL-13* genes (69, 70), which are genes known to regulate Th2 inflammation in asthma, complicate the interpretation of the importance of *KIF3A* alleles in the pathogenesis of atopy and asthma. Although the present studies do not exclude the possibility that asthma susceptibility related to this chromosomal region is associated with the other genes in that locus, present findings in our mouse models demonstrate a direct role for KIF3A in the regulation of aeroallergen-induced Th2 inflammation, airway epithelial repair, and mucociliary clearance, processes that may influence susceptibility to asthma.

Acknowledgments

We thank Shawn Grant, Jaymi Semona, Kalpana Srivastava, Brandy Ruff, Mehari E. Mengistu, Gail Macke, and Courtney Stockman for scientific assistance, Ann Maher for typing and editing on this manuscript, and the Cincinnati Children's Hospital Medical Center Viral Vector Core for making the lentiviruses.

Disclosures

The authors have no financial conflicts of interest.

References

1. Lambrecht, B. N., and H. Hammad. 2014. Allergens and the airway epithelium response: gateway to allergic sensitization. *J. Allergy Clin. Immunol.* 134: 499–507.
2. Rastogi, D., S. Fraser, J. Oh, A. M. Huber, Y. Schulman, R. H. Bhagtani, Z. S. Khan, L. Tesfa, C. B. Hall, and F. Macian. 2015. Inflammation, metabolic dysregulation, and pulmonary function among obese urban adolescents with asthma. *Am. J. Respir. Crit. Care Med.* 191: 149–160.
3. Corren, J., R. F. Lemanske, N. A. Hanania, P. E. Korenblat, M. V. Parsey, J. R. Arron, J. M. Harris, H. Scheerens, L. C. Wu, Z. Su, et al. 2011. Lebrikizumab treatment in adults with asthma. *N. Engl. J. Med.* 365: 1088–1098.
4. Jia, G., R. W. Erickson, D. F. Choy, S. Mosesova, L. C. Wu, O. D. Solberg, A. Shikotra, R. Carter, S. Audusseau, Q. Hamid, et al.; Bronchoscopic Exploratory Research Study of Biomarkers in Corticosteroid-refractory Asthma (BOBCAT) Study Group. 2012. Periostin is a systemic biomarker of eosinophilic airway inflammation in asthmatic patients. *J. Allergy Clin. Immunol.* 130: 647–654.e10.
5. Woodruff, P. G., B. Modrek, D. F. Choy, G. Jia, A. R. Abbas, A. Ellwanger, L. L. Koth, J. R. Arron, and J. V. Fahy. 2009. T-helper type 2-driven inflammation defines major subphenotypes of asthma. *Am. J. Respir. Crit. Care Med.* 180: 388–395.
6. Edwards, M. R., N. W. Bartlett, T. Hussell, P. Openshaw, and S. L. Johnston. 2012. The microbiology of asthma. *Nat. Rev. Microbiol.* 10: 459–471.
7. Parnia, S., J. L. Brown, and A. J. Frew. 2002. The role of pollutants in allergic sensitization and the development of asthma. *Allergy* 57: 1111–1117.
8. Kontakioti, E., K. Domvri, D. Papakosta, and M. Daniilidis. 2014. HLA and asthma phenotypes/endotypes: a review. *Hum. Immunol.* 75: 930–939.
9. Martinez, F. D., and D. Vercelli. 2013. Asthma. *Lancet* 382: 1360–1372.
10. Hill, M. R., and W. O. Cookson. 1996. A new variant of the β subunit of the high-affinity receptor for immunoglobulin E (FcεRI-β E237G): associations with measures of atopy and bronchial hyper-responsiveness. *Hum. Mol. Genet.* 5: 959–962.
11. Hirota, T., A. Takahashi, M. Kubo, T. Tsunoda, K. Tomita, M. Sakashita, T. Yamada, S. Fujieda, S. Tanaka, S. Doi, et al. 2012. Genome-wide association study identifies eight new susceptibility loci for atopic dermatitis in the Japanese population. *Nat. Genet.* 44: 1222–1226.
12. Kang, Z., Q. Li, P. Fu, S. Yan, M. Guan, J. Xu, and F. Xu. 2015. Correlation of KIF3A and OVOL1, but not ACTL9, with atopic dermatitis in Chinese pediatric patients. *Gene* 571: 249–251.
13. Lepre, T., R. Cascella, M. Ragazzo, E. Galli, G. Novelli, and E. Giardina. 2013. Association of KIF3A, but not OVOL1 and ACTL9, with atopic eczema in Italian patients. *Br. J. Dermatol.* 168: 1106–1108.
14. Paternoster, L., M. Standl, C. M. Chen, A. Ramasamy, K. Bønnelykke, L. Duijts, M. A. Ferreira, A. C. Alves, J. P. Thyssen, E. Albrecht, et al; Australian Asthma Genetics Consortium (AAGC); Genetics of Overweight Young Adults (GOYA) Consortium; EArly Genetics & Lifecourse Epidemiology (EAGLE) Consortium. 2011. Meta-analysis of genome-wide association studies identifies three new risk loci for atopic dermatitis. *Nat. Genet.* 44: 187–192.
15. Kim, J. H., J. Y. Cha, H. S. Cheong, J. S. Park, A. S. Jang, S. T. Uh, M. K. Kim, I. S. Choi, S. H. Cho, B. L. Park, et al. 2011. *KIF3A*, a cilia structural gene on chromosome 5q31, and its polymorphisms show an association with aspirin hypersensitivity in asthma. *J. Clin. Immunol.* 31: 112–121.
16. Kovacic, M. B., J. M. Myers, N. Wang, L. J. Martin, M. Lindsey, M. B. Ericksen, H. He, T. L. Patterson, T. M. Baye, D. Torgerson, et al. 2011. Identification of KIF3A as a novel candidate gene for childhood asthma using RNA expression and population allelic frequencies differences. *PLoS One* 6: e23714.
17. Hirokawa, N. 2000. Stirring up development with the heterotrimeric kinesin KIF3. *Traffic* 1: 29–34.
18. Hirokawa, N., Y. Noda, Y. Tanaka, and S. Niwa. 2009. Kinesin superfamily motor proteins and intracellular transport. *Nat. Rev. Mol. Cell Biol.* 10: 682–696.
19. Kodani, A., M. Salomé Sirerol-Piquer, A. Seol, J. M. Garcia-Verdugo, and J. F. Reiter. 2013. Kif3a interacts with dynactin subunit $p150^{Glued}$ to organize centriole subdistal appendages. *EMBO J.* 32: 597–607.
20. Lin, F., T. Hiesberger, K. Cordes, A. M. Sinclair, L. S. Goldstein, S. Somlo, and P. Igarashi. 2003. Kidney-specific inactivation of the KIF3A subunit of kinesin-II inhibits renal ciliogenesis and produces polycystic kidney disease. *Proc. Natl. Acad. Sci. USA* 100: 5286–5291.
21. Marszalek, J. R., P. Ruiz-Lozano, E. Roberts, K. R. Chien, and L. S. Goldstein. 1999. Situs inversus and embryonic ciliary morphogenesis defects in mouse mutants lacking the KIF3A subunit of kinesin-II. *Proc. Natl. Acad. Sci. USA* 96: 5043–5048.
22. Takeda, S., Y. Yonekawa, Y. Tanaka, Y. Okada, S. Nonaka, and N. Hirokawa. 1999. Left-right asymmetry and kinesin superfamily protein KIF3A: new insights in determination of laterality and mesoderm induction by $kif3A^{-/-}$ mice analysis. *J. Cell Biol.* 145: 825–836.
23. Goetz, S. C., and K. V. Anderson. 2010. The primary cilium: a signalling centre during vertebrate development. *Nat. Rev. Genet.* 11: 331–344.
24. Lancaster, M. A., and J. G. Gleeson. 2009. The primary cilium as a cellular signaling center: lessons from disease. *Curr. Opin. Genet. Dev.* 19: 220–229.
25. Quinlan, R. J., J. L. Tobin, and P. L. Beales. 2008. Modeling ciliopathies: primary cilia in development and disease. *Curr. Top. Dev. Biol.* 84: 249–310.
26. Veland, I. R., A. Awan, L. B. Pedersen, B. K. Yoder, and S. T. Christensen. 2009. Primary cilia and signaling pathways in mammalian development, health and disease. *Nephron Physiol.* 111: p39–53.
27. Boehlke, C., F. Kotsis, B. Buchholz, C. Powelske, K. U. Eckardt, G. Walz, R. Nitschke, and E. W. Kuehn. 2013. Kif3a guides microtubular dynamics, migration and lumen formation of MDCK cells [Published erratum appears in 2013 *PLoS One* 8: e62165]. *PLoS One* 8: e62165.
28. Boehlke, C., F. Kotsis, V. Patel, S. Braeg, H. Voelker, S. Bredt, T. Beyer, H. Janusch, C. Hamann, M. Gödel, et al. 2010. Primary cilia regulate mTORC1 activity and cell size through Lkb1. *Nat. Cell Biol.* 12: 1115–1122.
29. Carpenter, B. S., R. L. Barry, K. J. Verhey, and B. L. Allen. 2015. The heterotrimeric kinesin-2 complex interacts with and regulates GLI protein function. *J. Cell Sci.* 128: 1034–1050.
30. Qiu, N., Z. Xiao, L. Cao, M. M. Buechel, V. David, E. Roan, and L. D. Quarles. 2012. Disruption of Kif3a in osteoblasts results in defective bone formation and osteopenia. *J. Cell Sci.* 125: 1945–1957.
31. Sipe, C. W., and X. Lu. 2011. Kif3a regulates planar polarization of auditory hair cells through both ciliary and non-ciliary mechanisms. *Development* 138: 3441–3449.
32. Haycraft, C. J., Q. Zhang, B. Song, W. S. Jackson, P. J. Detloff, R. Serra, and B. K. Yoder. 2007. Intraflagellar transport is essential for endochondral bone formation. *Development* 134: 307–316.
33. Ji, H., A. M. Houghton, T. J. Mariani, S. Perera, C. B. Kim, R. Padera, G. Tonon, K. McNamara, L. A. Marconcini, A. Hezel, et al. 2006. K-ras activation generates an inflammatory response in lung tumors. *Oncogene* 25: 2105–2112.
34. Harfe, B. D., P. J. Scherz, S. Nissim, H. Tian, A. P. McMahon, and C. J. Tabin. 2004. Evidence for an expansion-based temporal Shh gradient in specifying vertebrate digit identities. *Cell* 118: 517–528.
35. Delmotte, P., and M. J. Sanderson. 2006. Ciliary beat frequency is maintained at a maximal rate in the small airways of mouse lung slices. *Am. J. Respir. Cell Mol. Biol.* 35: 110–117.
36. Francis, R., and C. Lo. 2013. Ex vivo method for high resolution imaging of cilia motility in rodent airway epithelia. *J. Vis. Exp.* 78: e50343. Available at: https://www.jove.com/video/50343/ex-vivo-method-for-high-resolution-imaging-cilia-motility-rodent.
37. Li, B. W., and R. W. Hendriks. 2013. Group 2 innate lymphoid cells in lung inflammation. *Immunology* 140: 281–287.
38. Rajavelu, P., G. Chen, Y. Xu, J. A. Kitzmiller, T. R. Korfhagen, and J. A. Whitsett. 2015. Airway epithelial SPDEF integrates goblet cell differentiation and pulmonary Th2 inflammation. *J. Clin. Invest.* 125: 2021–2031.

Downloaded from http://www.jimmunol.org/ at Liverpool University Library on December 12, 2016

39. Davidovich, N., B. C. DiPaolo, G. G. Lawrence, P. Chhour, N. Yehya, and S. S. Margulies. 2013. Cyclic stretch-induced oxidative stress increases pulmonary alveolar epithelial permeability. *Am. J. Respir. Cell Mol. Biol.* 49: 156–164.
40. Du, Y., M. Guo, J. A. Whitsett, and Y. Xu. 2015. "LungGENS": a web-based tool for mapping single-cell gene expression in the developing lung. *Thorax* 70: 1092–1094.
41. Jain, R., J. Pan, J. A. Driscoll, J. W. Wisner, T. Huang, S. P. Gunsten, Y. You, and S. L. Brody. 2010. Temporal relationship between primary and motile ciliogenesis in airway epithelial cells. *Am. J. Respir. Cell Mol. Biol.* 43: 731–739.
42. Harris, K. S., Z. Zhang, M. T. McManus, B. D. Harfe, and X. Sun. 2006. Dicer function is essential for lung epithelium morphogenesis. *Proc. Natl. Acad. Sci. USA* 103: 2208–2213.
43. Gilley, S. K., A. E. Stenbit, R. C. Pasek, K. M. Sas, S. L. Steele, M. Amria, M. A. Bunni, K. P. Estell, L. M. Schwiebert, P. Flume, et al. 2014. Deletion of airway cilia results in noninflammatory bronchiectasis and hyperreactive airways. *Am. J. Physiol. Lung Cell. Mol. Physiol.* 306: L162–L169.
44. Pazour, G. J., B. L. Dickert, Y. Vucica, E. S. Seeley, J. L. Rosenbaum, G. B. Witman, and D. G. Cole. 2000. *Chlamydomonas IFT88* and its mouse homologue, polycystic kidney disease gene *Tg737*, are required for assembly of cilia and flagella. *J. Cell Biol.* 151: 709–718.
45. Buckpitt, A., A. M. Chang, A. Weir, L. Van Winkle, X. Duan, R. Philpot, and C. Plopper. 1995. Relationship of cytochrome P450 activity to Clara cell cytotoxicity. IV. Metabolism of naphthalene and naphthalene oxide in microdissected airways from mice, rats, and hamsters. *Mol. Pharmacol.* 47: 74–81.
46. Shultz, M. A., D. Morin, A. M. Chang, and A. Buckpitt. 2001. Metabolic capabilities of CYP2F2 with various pulmonary toxicants and its relative abundance in mouse lung subcompartments. *J. Pharmacol. Exp. Ther.* 296: 510–519.
47. Hammad, H., and B. N. Lambrecht. 2015. Barrier epithelial cells and the control of type 2 immunity. *Immunity* 43: 29–40.
48. Sehgal, I. S., S. Dhooria, A. Bal, and R. Agarwal. 2015. Allergic bronchopulmonary aspergillosis in an adult with Kartagener syndrome. *BMJ Case Rep.* DOI: 10.1136/bcr-2015-211493.
49. Sharma, B., M. Sharma, E. Bondi, and M. Sharma. 2005. Kartagener's syndrome associated with allergic bronchopulmonary aspergillosis. *MedGenMed* 7: 25.
50. Balenga, N. A., M. Klichinsky, Z. Xie, E. C. Chan, M. Zhao, J. Jude, M. Laviolette, R. A. Panettieri, Jr., and K. M. Druey. 2015. A fungal protease allergen provokes airway hyper-responsiveness in asthma. *Nat. Commun.* 6: 6763.
51. Perkins, C., N. Yanase, G. Smulian, L. Gildea, T. Orekov, C. Potter, F. Brombacher, B. Aronow, M. Wills-Karp, and F. D. Finkelman. 2011. Selective stimulation of IL-4 receptor on smooth muscle induces airway hyperresponsiveness in mice. *J. Exp. Med.* 208: 853–867.
52. Damera, G., O. Tliba, and R. A. Panettieri, Jr. 2009. Airway smooth muscle as an immunomodulatory cell. *Pulm. Pharmacol. Ther.* 22: 353–359.
53. Georas, S. N., and F. Rezaee. 2014. Epithelial barrier function: at the front line of asthma immunology and allergic airway inflammation. *J. Allergy Clin. Immunol.* 134: 509–520.
54. Heijink, I. H., M. C. Nawijn, and T. L. Hackett. 2014. Airway epithelial barrier function regulates the pathogenesis of allergic asthma. *Clin. Exp. Allergy* 44: 620–630.
55. Bush, A., and C. Hogg. 2012. Primary ciliary dyskinesia: recent advances in epidemiology, diagnosis, management and relationship with the expanding spectrum of ciliopathy. *Expert Rev. Respir. Med.* 6: 663–682.
56. Leigh, M. W., J. E. Pittman, J. L. Carson, T. W. Ferkol, S. D. Dell, S. D. Davis, M. R. Knowles, and M. A. Zariwala. 2009. Clinical and genetic aspects of primary ciliary dyskinesia/Kartagener syndrome. *Genet. Med.* 11: 473–487.
57. Guajardo, J. R., K. W. Schleifer, M. O. Daines, R. M. Ruddy, B. J. Aronow, M. Wills-Karp, and G. K. Hershey. 2005. Altered gene expression profiles in nasal respiratory epithelium reflect stable versus acute childhood asthma. *J. Allergy Clin. Immunol.* 115: 243–251.
58. Thomas, B., A. Rutman, R. A. Hirst, P. Haldar, A. J. Wardlaw, J. Bankart, C. E. Brightling, and C. O'Callaghan. 2010. Ciliary dysfunction and ultrastructural abnormalities are features of severe asthma. *J. Allergy Clin. Immunol.* 126:722–729.e2.
59. Dagenais, T. R., and N. P. Keller. 2009. Pathogenesis of *Aspergillus fumigatus* in invasive aspergillosis. *Clin. Microbiol. Rev.* 22: 447–465.
60. Gregory, L. G., and C. M. Lloyd. 2011. Orchestrating house dust mite-associated allergy in the lung. *Trends Immunol.* 32: 402–411.
61. Fahy, J. V. 2015. Type 2 inflammation in asthma—present in most, absent in many. *Nat. Rev. Immunol.* 15: 57–65.
62. Lambrecht, B. N., and H. Hammad. 2013. Asthma: the importance of dysregulated barrier immunity. *Eur. J. Immunol.* 43: 3125–3137.
63. Erle, D. J., and D. Sheppard. 2014. The cell biology of asthma. *J. Cell Biol.* 205: 621–631.
64. Chen, G., T. R. Korfhagen, C. L. Karp, S. Impey, Y. Xu, S. H. Randell, J. Kitzmiller, Y. Maeda, H. M. Haitchi, A. Sridharan, et al. 2014. Foxa3 induces goblet cell metaplasia and inhibits innate antiviral immunity. *Am. J. Respir. Crit. Care Med.* 189: 301–313.
65. Chen, G., T. R. Korfhagen, Y. Xu, J. Kitzmiller, S. E. Wert, Y. Maeda, A. Gregorieff, H. Clevers, and J. A. Whitsett. 2009. SPDEF is required for mouse pulmonary goblet cell differentiation and regulates a network of genes associated with mucus production. *J. Clin. Invest.* 119: 2914–2924.
66. Veland, I. R., L. Lindbæk, and S. T. Christensen. 2014. Linking the primary cilium to cell migration in tissue repair and brain development. *Bioscience* 64: 1115–1125.
67. Blitzer, A. L., L. Panagis, G. L. Gusella, J. Danias, M. Mlodzik, and C. Iomini. 2011. Primary cilia dynamics instruct tissue patterning and repair of corneal endothelium. *Proc. Natl. Acad. Sci. USA* 108: 2819–2824.
68. Boehlke, C., H. Janusch, C. Hamann, C. Powelske, M. Mergen, H. Herbst, F. Kotsis, R. Nitschke, and E. W. Kuehn. 2015. A cilia independent role of Ift88/polaris during cell migration. *PLoS One* 10: e0140378.
69. Cousins, D. J., T. H. Lee, and D. Z. Staynov. 2002. Cytokine coexpression during human Th1/Th2 cell differentiation: direct evidence for coordinated expression of Th2 cytokines. *J. Immunol.* 169: 2498–2506.
70. Frazer, K. A., Y. Ueda, Y. Zhu, V. R. Gifford, M. R. Garofalo, N. Mohandas, C. H. Martin, M. J. Palazzolo, J. F. Cheng, and E. M. Rubin. 1997. Computational and biological analysis of 680 kb of DNA sequence from the human 5q31 cytokine gene cluster region. *Genome Res.* 7: 495–512.

Downloaded from http://www.jimmunol.org/ at Liverpool University Library on December 12, 2016

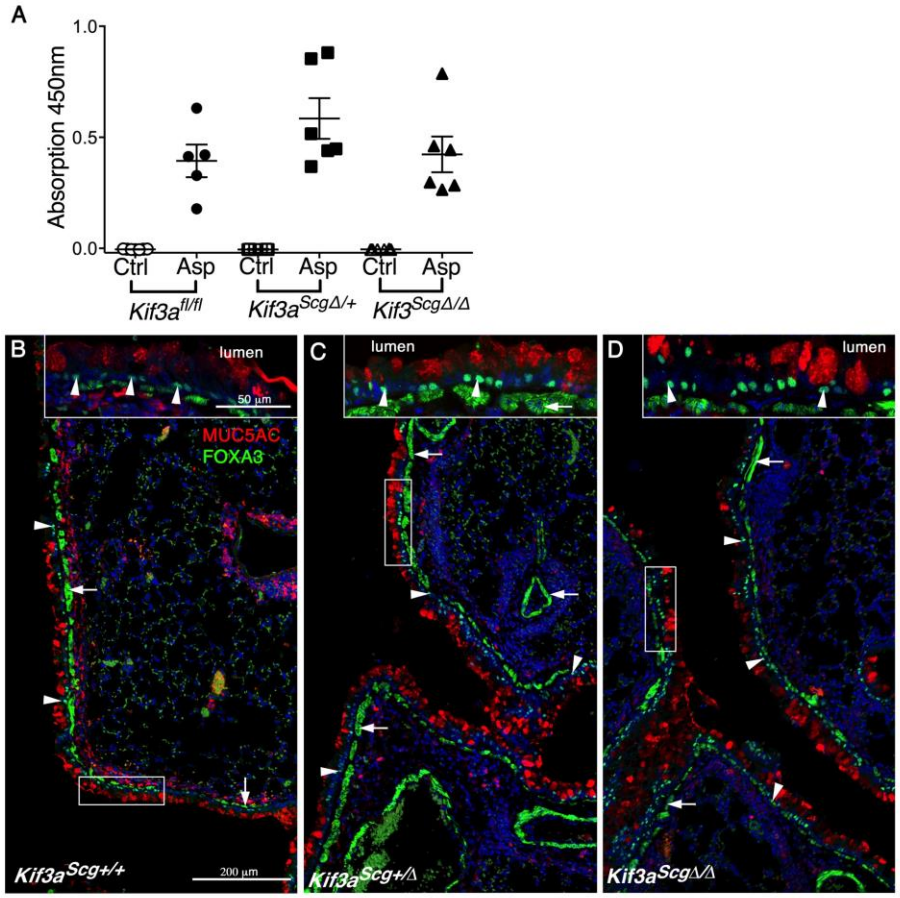

Supplement Figure 1. Aspergillus sensitization in *Kif3a* gene deleted mice. Aspergillus specific IgG1 ELISA assays indicated no differences in the response between the genotypes of aspergillus exposed animals. Data are represented as Mean±SEM with n=5-7 in each group (A). Goblet cell markers, MUC5AC (red) and FOXA3 (green nuclei indicated by arrowheads), were expressed in mice of all *Kif3a* genotypes following exposure to *Aspergillus* extract (B-D). Note non-specific green staining of smooth muscle, arrows (B-D). Small boxes indicate regions shown in insets.

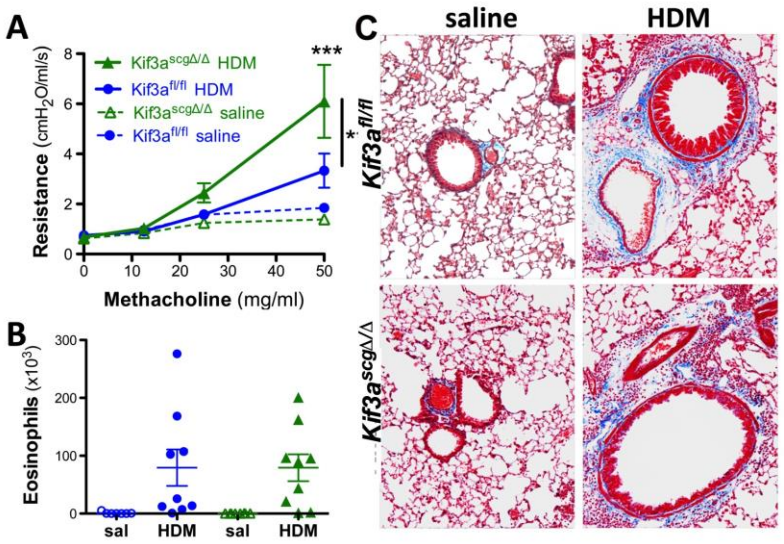

Supplement Figure 2. Increased AHR in house dust mite exposed *Kif3a* gene deleted mice. Aged-matched *Kif3a* gene deficient (*Kif3a*$^{Scg\Delta/\Delta}$) and sufficient (*Kif3a*$^{fl/fl}$) mice were exposed to either saline or house dust mite extract. AHR was assessed by measuring lung resistance to increasing doses of methacholine (A). Data represent the mean±SEM of 5-8 mice per group. Significance was assessed by 2-way ANOVA (**p<0.01, ***p<0.001). Total BALF eosinophil numbers were not significantly different between HDM treated animals (B). Representative images of lung sections stained with trichrome (C).

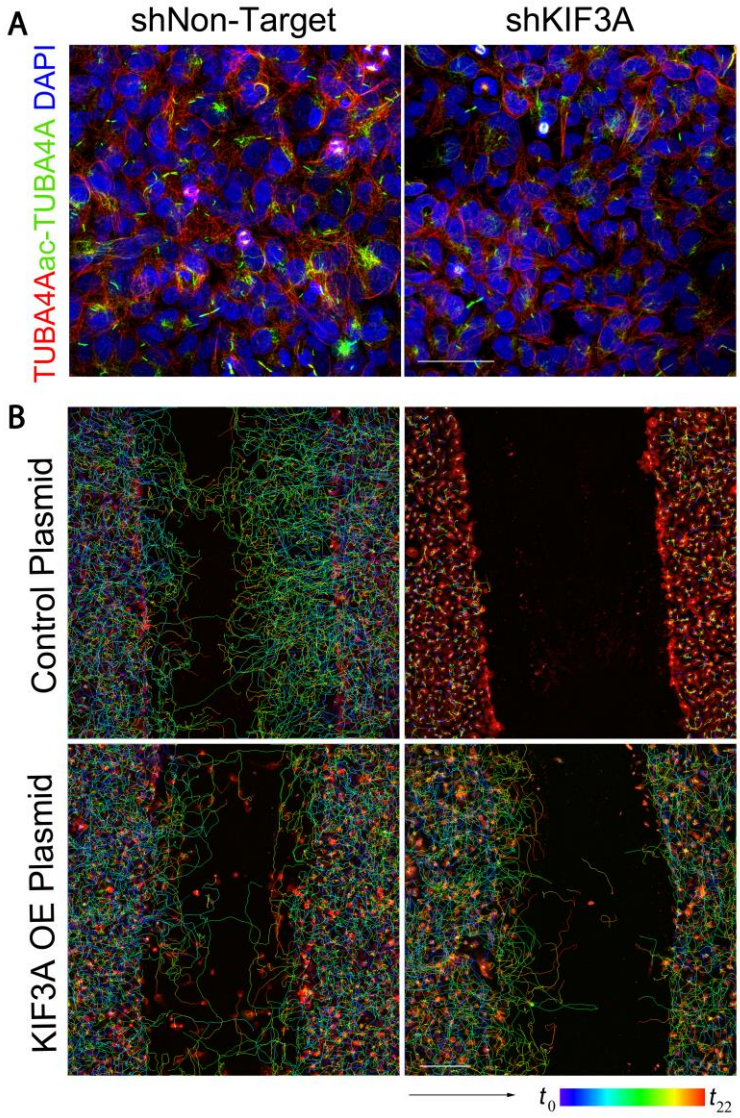

Supplement Figure 3. BEAS2B cells were transduced with scramble control or KIF3A shRNA lentivirus. Loss of KIF3A was associated with disruption of microtubules as observed by acetylated tubulin immunofluorescence staining. Data are representative of n=2 experiments (A). HBEC3 cells were stained with di-8-ANEPPS and the monolayer was wounded by mechanical scratch. Cell migration was impaired in shKIF3A transduced cells as observed by videography over 22 hours. Cell tracking analysis showed that inhibition of KIF3A affected migration trajectory characteristics such as displacement, directionality, speed and persistence of movement which was rescued by expressing full-length KIF3A cDNA construct (B).

Legends for Videos:

Video 1 and Video 2. Cell migration. HBEC3 and BEAS2B cells were transduced with control and KIF3A shRNA lenti-viruses. Timelapse imaging videos of cell migration in scratch assays were captured for a duration of 14-16 hours for HBEC3 cells (Video 1) and BEAS-2B cells (Video 2), showing that knockdown of *KIF3A* suppresses cell migration.

Video 3 and Video 4. Ciliary beating and tracheal flow. DIC movie of tracheal mounts of $Kif3a^{Shh\Delta/+}$, $Kif3a^{Shh\Delta/\Delta}$ and controls collected at 500 frames/second (fps) and playback at 30fps (Video 3). Cilia generated flow images were collected at 200fps and playback at 30fps (Video 4). Similar loss of ciliary beat and directional movement was observed in large airways of $Kif3a^{Scg\Delta/\Delta}$ mice, not shown.